STIFTELSEN BERGTEKNISK FORSKNING
ROCK ENGINEERING RESEARCH FOUNDATION

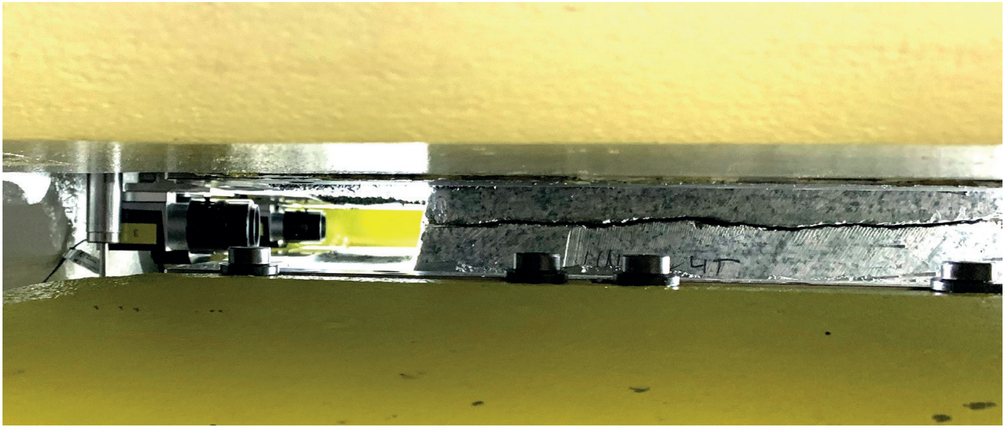

ON ACCURACY IN DIRECT SHEAR TESTING OF ROCK JOINTS – Impact of joint type, boundary conditions and joint size

Jörgen Larsson

BeFo Report 251

Cover photo: Deformation measurement across a rock joint under load with conventional position sensors and digital image analysis simultaneously. Photo: Jörgen Larsson.

STIFTELSEN BERGTEKNISK FORSKNING
ROCK ENGINEERING RESEARCH FOUNDATION

ON ACCURACY IN DIRECT SHEAR TESTING OF ROCK JOINTS - Impact of joint type, boundary conditions and joint size

Om noggrannhet vid direkta skjuvtester på bergssprickor – Beroenden av spricktyp, randvillkor och sprickstorlek

Jörgen Larsson

BeFo Report 251
Stockholm 2025
ISSN 1104-1773
ISRN BEFO-R-251-SE

This report is in parts a copy of a Doctoral Thesis in Civil and Architectural Engineering, Soil and Rock Mechanics, published by KTH Royal Institute of Technology, Stockholm, Sweden 2025: “Approaches for increased accuracy in laboratory direct shear testing of rock joints”. © Jörgen Larsson, ISBN 978-91-8106-205-2. TRITA-ABE-DLT-251. This BeFo report is published with the permission of the author.

PREFACE

Rock joints influence the stability of rock mass. Therefore, their shear strength is an important factor in determining the load a structure constructed on or in rock can withstand. Numerical and theoretical models are typically used to predict the shear mechanical behaviour of the rock mass as well as the rock joints and these models are validated based on laboratory testing.

The data generation process from laboratory testing consists of several parts, each of which is associated with various sources of uncertainties. However, no model is better than the accuracy of the results it is validated against. Therefore, in this work, several approaches have been developed using data from a comprehensive experimental shear testing program, with the overall aim of reducing the uncertainties associated with various parts of the process.

The work is part of an PhD study conducted at KTH under the supervision of Fredrik Johansson and Diego Mas Ivars with additional support from Erland Johnson, Lars Jacobsson, Mathias Flansbjer and from a reference group consisting of Christer Andersson, Axel Bolin, Mattias Roslin, Per Tengborg, Patrik Vidstrand and Thomas Wettainen.

The research has been co-funded by SKB (Swedish Nuclear Fuel and Waste Management Co, Sweden) and NWMO (Nuclear Waste Management Organization, Canada), RISE, KTH and BeFo.

FÖRORD

Bergssprickor påverkar stabiliteten hos bergmassan. Därför är deras skjuvhållfasthet viktig för att bestämma den belastning en struktur som byggts på eller i berg kan tåla. Numeriska och teoretiska modeller används vanligtvis för att förutsäga det mekaniska beteendet hos bergmassan respektive sprickorna, och dessa modeller valideras utifrån laboratorietester.

Datagenereringsprocessen vid laboratorietester består av flera delar, var och en kopplad till olika källor till osäkerhet och ingen modell är bättre än noggrannheten hos de resultat den valideras mot. Därför har metoder utvecklats i detta arbete med hjälp av data från ett omfattande experimentellt testprogram, med det övergripande syftet att minska osäkerheterna kopplade till de olika delarna av processen.

Arbetet är en del av en doktorsavhandling genomförd vid KTH under överinseende av Fredrik Johansson och Diego Mas Ivars med ytterligare stöd från Erland Johnson, Lars Jacobsson, Mathias Flansbjer och från en referensgrupp bestående av Christer Andersson, Axel Bolin, Mattias Roslin, Per Tengborg, Patrik Vidstrand och Thomas Wettainen.

Forskningen har delvis finansierats av SKB (Svensk Kärnbränslehantering AB, Sverige) och NWMO (Nuclear Waste Management Organization, Kanada), RISE, KTH och BeFo.

SUMMARY

Rock joints influence the stability of rock mass. Therefore, their shear strength is an important factor in determining the load a structure constructed on or in rock can withstand. Numerical and theoretical models are used to predict the shear mechanical behaviour of rock joints. These models are validated against data from laboratory testing. The data generation process from laboratory testing consists of several parts, each of which is associated with various sources of uncertainties. However, no model is better than the accuracy of the results it is validated against. Therefore, in this work, several approaches have been developed using data from a comprehensive experimental shear testing program, with the overall aim of reducing the uncertainties associated with various parts of the data generation process.

Forty-six granite rock specimens containing both natural and artificially tensile induced joints were subjected to direct shear testing. Several tests were carried out for each parameter combination, allowing for statistical evaluations. The tests were conducted under controlled laboratory conditions under both constant normal stress and constant normal stiffness boundary conditions. These tests were performed under previously unexplored conditions, combining stresses occurring at depths of several hundreds of meters with a wide range of joint areas represented across three specimen sizes: 35 mm × 60 mm, 70 mm × 100 mm and 300 mm × 500 mm. In addition, fifteen replicas were manufactured from high-strength concrete based on one of the granite rock joints sized 70 mm × 100 mm for geometrical evaluations. Six of these replicas were subjected to direct shear testing and evaluated against the shear mechanical behaviour of the rock joint.

Two quality assurance parameters for replica rock joints have been developed, which together with a method for establishing threshold limits of the parameters, reduces the uncertainties in parametric studies. An approach has been developed in which the effective normal stiffness is calculated and then inserted into the control system in tests under the constant normal stiffness boundary condition. The application of the effective normal stiffness essentially eliminates the error in applied normal load originating from the normal stiffness of the test system. Improved accuracy in displacement measurements has been achieved by applying optical displacement measurements directly over joint traces. Direct displacement measurements exclude errors in conventional measurements, which include undesired but unavoidable displacements originating from gaps and deformations in the test system. Approaches for consistent and physically based determination of both shear strength and shear stiffness have been developed. Analysis of variance shows that the shear strength of the tested rock joint specimens is not influenced by specimen size, whereas shear stiffness is. To sum up, the accuracy of data from laboratory tests is improved, constituting a prerequisite for improved models.

Keywords: Displacement measurement, Scale effect, Stiffness, Shear strength, Uncertainty

SAMMANFATTNING

Bergssprickor påverkar bergmassans stabilitet. Bergssprickors skjuvhållfasthet utgör därför en betydande faktor för vilka laster en berganläggning skall dimensioneras för. Numeriska och teoretiska modeller används för att prediktera bergssprickors skjuvhållfasthet. Modellerna valideras mot data från laboratorietester. Processen att ta fram data från laboratorietester består av flera delar, vilka var och en innehåller olika typer av osäkerheter. Inga modeller är dock bättre än noggrannheten på resultaten de valideras mot. Med hjälp av data från ett omfattande experimentellt testprogram har därför ett antal tillvägagångssätt utvecklats, vilka syftar till att minska osäkerheterna inom olika delar av dataframtagningsprocessen.

Direkta skjuvtester utfördes på fyrtiosex bergprov av granit med både naturliga och artificiellt spänningsinducerade sprickor. Flera tester utfördes för varje parameterkombination, vilket möjliggjorde statistiska utvärderingar. Testerna utfördes i kontrollerad laboratoriemiljö under både konstant normalspänning och konstant normalstyvhet. Dessa tester utfördes under förhållanden som inte studerats tidigare genom kombinationen av spänningar motsvarande djup på flera hundra meter och en bred fördelning av sprickareor representerade av tre provkroppsstorlekar: 35 mm × 60 mm, 70 mm × 100 mm and 300 mm × 500 mm. Dessutom tillverkades femton repliker av höghållfast betong från en av granitsprickorna med storleken 70 mm × 100 mm för geometriska utvärderingar. Sex av dessa repliker genomgick direkta skjuvtester och deras skjuvmekaniska beteende utvärderades mot bergssprickans.

Två kvalitetssäkringsparametrar för replikers sprickgeometri har tagits fram, vilka tillsammans med en metod för framtagning av parametergränsvärden reducerar osäkerheten i parameterstudier. Ett tillvägagångssätt har utvecklats där den effektiva normalstyvheten först beräknas och därefter anges som styrparameter i tester under randvillkoret konstant normalstyvhet. Den effektiva normalstyvheten eliminerar i princip felet i pålagd normallast orsakad av testsystemets normalstyvhet. Förbättrad noggrannhet vid förskjutningsmätningar har uppnåtts genom tillämpning av optiska förskjutningsmätningar direkt över sprickprofiler. Direkta mätningar eliminerar felen i konventionella mätningar, vilka inkluderar oönskade, men oundvikliga, bidrag härrörande från glapp och deformationer i testsystemet. Tillvägagångssätt som möjliggör konsistent och fysikaliskt baserad framtagning av både skjuvhållfasthet och skjuvstyvhet har tagits fram. Variansanalys visar att skjuvhållfastheten för de testade bergproven inte påverkas av provstorleken, medan skjuvstyvheten gör det. Sammantaget skapas förbättrad noggrannhet i data från laboratorietester av bergssprickor, vilket utgör en grund för förbättrade modeller för att prediktera deras skjuvhållfasthet.

Nyckelord: Förskjutningsmätning, Skaleffekt, Styvhet, Skjuvhållfasthet, Osäkerhet

LIST OF ABBREVIATIONS[1]

i	Numbering index
k_{eff}	Effective normal stiffness
k_{ns}	Intended normal stiffness
k_{sys}	System normal stiffness
N	Number of coordinate points
t	Time
$\boldsymbol{V}$	Normal vector to the best-fit plane to be evaluated
$\boldsymbol{V}_{Hp100}$	Projected vector capturing deviations with respect to specimen holder position (shear direction)
$\boldsymbol{V}_{RP}$	Normal vector to the reference best-fit plane
$\boldsymbol{V}_1$	The orthogonal projection of $\boldsymbol{V}$ onto $\boldsymbol{V}_{RP}$
$\boldsymbol{V}_2$	The orthogonal projection of $\boldsymbol{V}$ onto Π_{RP}
w	Weight
α	Angle of inclination
α_i	Factor representing joint type
β_j	Factor representing boundary condition
γ	Angle [$\boldsymbol{V}$, $\boldsymbol{V}_{Hp100}$]
γ_k	Factor representing specimen size
δ_n	Normal displacement
δ_{n_nom}	Nominal normal displacement
δ_s	Shear displacement
$\dot{\delta}_{s\_const}$	The time interval for determining the shear stiffness, during which first-time derivative of shear displacement is constant

[1] Symbols in the equations from the literature in Section 1.2 are not included

$\ddot{\delta}_{\mathrm{s0}}$	The point of time when the second-time derivative of the shear displacement equals zero
$\varepsilon_{\mathrm{ijkl}}$	Error term
ζ_{i}	Deviation value along the evaluation direction for the i:th coordinate point
$\bar{\zeta}$	Mean of the deviations of the coordinate points along the evaluation direction
μ	Mean shear strength
Π	Best-fit plane to be evaluated
Π_{RP}	Reference best-fit plane
σ_{n}	Normal stress
σ_{n0}	Initial normal stress
σ_{mf}	Quality assurance parameter with respect to morphology
τ	Shear stress
$\tau_{\mathrm{p\_ijkl}}$	Shear strength

CONTENTS

1. INTRODUCTION

1.1 Background

Having control of the load bearing capacity of a rock mass is of importance for several reasons. Increased construction efficiency reduced negative environmental impact, safer urban transportation systems and more robust infrastructure follows from increased control of load bearing capacity. Moreover, the working environment during construction and operation is improved from better control of safety margins. Theoretical models are used for prediction of load bearing capacity. Both development and validation of theoretical models are done through testing of rock samples. Consequently, the accuracy of theoretical models cannot be better than the accuracy of the results from the tests of the samples. Accurate results from testing are therefore of fundamental importance.

Shearing of rock joints is critical for the stability of fractured rock masses. The presence of rock joints must thus be considered in the design of structures founded on or excavated in such rock masses. The development of shear strength criteria from in situ experiments is generally not feasible for both technical and economic reasons (Bandis et al. 1981). Shear strength criteria are therefore mainly validated against results from laboratory direct shear testing, e.g., Patton (1966), Barton (1973), Grasselli et al. (2003) and Casagrande et al. (2018) among others.

A project, POST (Parametrization Of STructures), was carried out during 2014 – 2016 aiming to develop knowledge about prediction of deformations of joints around a geological repository for spent nuclear fuel through in-situ testing and numerical modelling (Siren et al. 2017). Originating from technical challenges associated with in-situ tests, it was concluded that the uncertainties need to be reduced, which would require controlled laboratory direct shear testing of rock joints of different sizes under loading conditions representative of stress states at depths of several hundred meters.

A second phase of the POST project was launched in 2017 (Jacobsson et al., 2021 and Pérez Rey et al., 2024), within which a new direct shear test equipment was developed, allowing tests to be conducted with a unique combination of large loads (up to 5 MN) and large joint areas (up to 400 mm × 600 mm). The new direct shear test equipment was used in an extensive experimental project, addressing the uncertainties associated with previous studies and expanding the existing range of knowledge. This was achieved by testing different joint types under different boundary conditions, including previously unexplored conditions that combine stresses occurring at depths of several hundreds of meters, with a wide range of joint sizes represented across three specimen sizes. The results were analysed, and several approaches were developed to reduce the uncertainties associated with the data generation process. These approaches contribute to the overall objective of facilitating the development of improved criteria for predicting the shear mechanical behaviour of rock joints.

1.2 Theoretical modelling of rock joints

The shear strength characteristic of rock masses is governed by the existence of joints, i.e., pre-existing fractures. Shearing of rock joints is therefore a critical failure mode and must be taken into consideration in the design of structures founded on rock, such as dam foundations, or excavated in rock such as tunnels and caverns. Knowledge about the factors and mechanisms affecting shear mechanical behaviour is required for incorporating design safety margins and enhancing the serviceability of these structures. Shearing occurs under two types of boundary conditions. In, for example, slope stability problems, when the rock mass slides under the influence of its own weight, w, the load in terms of normal stress over the joint is constant. This state is denoted as the constant normal stress (CNL) boundary condition and is illustrated in Figure 1a. In underground excavations, when the stiffness of the surrounding rock mass, k_{ns}, constrains the dilation of the joint during shearing as illustrated in Figure 1b, the constant normal stiffness (CNS) boundary condition applies (Haberfield et al. 2003).

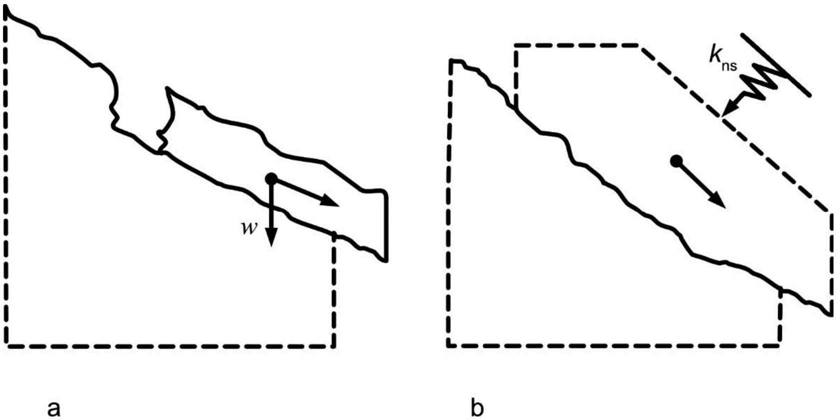

Figure 1. Conceptual illustration of the constant normal stress (CNL) (a), and the constant normal stiffness (CNS) (b) boundary conditions.

Several theoretical models predicting the shear mechanical behaviour of rock joints have been proposed. Common to all models is that both their development and validation of them rely on laboratory testing of rock samples. In the following, some theoretical models are described to illustrate examples of incorporated parameters.

1.2.1 Constant normal load

The first criterion relating shear stress to normal stress and dilatancy was introduced by Patton (1966). Under the CNL boundary condition and under low normal stresses, when sliding over asperities is presumed to be the predominant mode, the following expression was derived from laboratory tests on saw-tooth profiles

$$\tau = \sigma_n \cdot \tan(\emptyset_b + \acute{\imath}) \,, \tag{1}$$

in which τ is the shear stress, σ_n is the applied normal stress, $\emptyset_b$ is the basic friction angle, and $\acute{\imath}$ is the asperity angle, in this study, the inclination angle of the teeth (Figure 2).

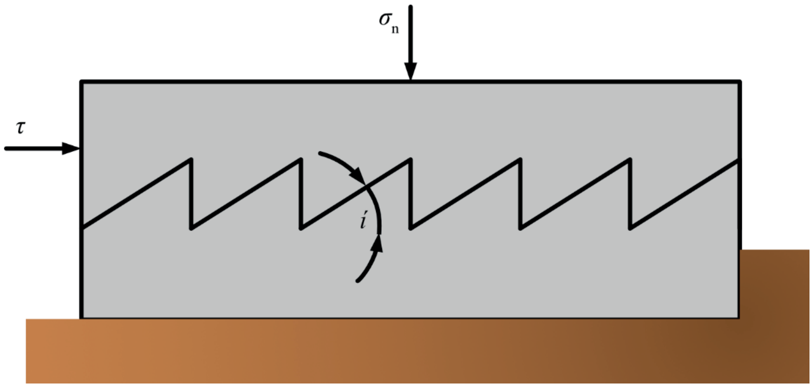

Figure 2. Illustration of the saw-toothed profile used by Patton (1966).

Barton et al. (1977) derived an empirical equation for predicting the peak shear strength, τ_p by substituting $\acute{\imath}$ in Eq. (1) with a term dependent on σ_n, the joint compressive strength (JCS) and the roughness of the joint surface expressed by the joint roughness coefficient (JRC), and by substituting $\emptyset_b$ with the residual friction angle ϕ_r

$$\tau_p = \sigma_n \cdot \tan\left(\phi_r + JRC \cdot Log_{10} \cdot \left(\frac{JCS}{\sigma_n}\right)\right). \tag{2}$$

Grasselli (2001) developed a model for predicting τ_p by incorporating the effect of surface morphology and the tensile strength of intact rock:

$$\tau_p = \sigma_n \cdot \tan(\phi_r) \cdot (1 + g), \tag{3}$$

where g is a term that quantifies the contribution of the joint morphology to τ_p. g is given by

$$g = e^{\frac{-\phi^*_{max}}{9 \cdot A_0 \cdot C} \cdot \frac{\sigma_n}{\sigma_t}}, \tag{4}$$

in which ϕ^*_{max} is the maximum apparent dip angle, A_0 is the maximum potential contact area, C is a roughness parameter, and σ_t is the tensile strength. In Eq. (3) ϕ_r is the residual shear strength after 5 mm shear displacement calculated as

$$\phi_{\mathrm{r}} = \phi_{\mathrm{b}} + \left(C \cdot A_0^{1.5} \cdot \phi_{max}^{*} \cdot \left(1 - A_0^{\frac{1}{C}} \right) \right)^{\cos \acute{\alpha}}, \tag{5}$$

in which $\acute{\alpha}$ is the angle between the schistosity plane and the normal to the joint. The term after the plus sign represents the contribution of the joint morphology to the residual friction angle.

Johansson et al. (2014) and Ríos-Bayona et al. (2021) incorporated the influence of joint matching and joint size through the following model predicting the peak friction angle ϕ_{p} as

$$\phi_{\mathrm{p}} = \phi_{\mathrm{b}} + i_{\mathrm{n}}, \tag{6}$$

in which

$$i_{\mathrm{n}} = \tan^{-1}\left(\tan(i_{\mathrm{g}}) \cdot \left(\frac{L_{\mathrm{n}}}{L_{\mathrm{g}}} \right)^{kH-k} \right), \tag{7}$$

in which

$$i_{\mathrm{g}} = \phi_{max}^{*} - 10^{\left(\frac{\log \frac{\sigma_{\mathrm{n}}}{\sigma_{\mathrm{ci}}} - \log A_0}{C} \right)} \cdot \phi_{max}^{*}, \tag{8}$$

and

$$k = \frac{\log \frac{2a}{\tan i_{\mathrm{n}}} - \log \frac{L_{asp.g}}{2}}{\log \frac{L_{\mathrm{n}}}{2} - \log \frac{L_{\mathrm{g}}}{2}}, \tag{9}$$

where L_{g} is the length at grain scale, L_{n} is the length of the sample, $L_{asp.g}$ is the size of the effective asperities at contact during shearing, H is the Hurst exponent (Yang et al. 1997), σ_{ci} is the uniaxial compressive strength of intact rock and a the average aperture.

Grasselli (2001) also suggested a linear relationship between τ_{p}, σ_{n} and the horizontal displacement before the peak shear strength, $\Delta\delta_{\mathrm{s\_peak}}$ in order to calculate shear stiffness, k_s

$$k_{\mathrm{s}} = \frac{1}{\Delta\delta_{\mathrm{s\_peak}}} \cdot \frac{\tau_{\mathrm{p}}}{\sigma_{\mathrm{n}}}, \tag{10}$$

in which

$$\Delta\delta_{\mathrm{s\_peak}} = \delta_{\mathrm{s\_peak}} - b, \tag{11}$$

where $\delta_{\mathrm{s\_peak}}$ is the total peak shear displacement and b the horizontal displacement required to get the joint mated.

Hossaini et al. (2014) incorporated the Young's modulus of intact rock E by suggesting the following equation

$$k_{\mathrm{s}} = \left(\frac{\sigma_{\mathrm{n}}}{\delta_{\mathrm{s\_peak}}}\right)^{a_1} \cdot \left(1 - \frac{E}{\sigma_{\mathrm{ci}}}\right)^{a_2} \cdot JRC^{a_3}, \tag{12}$$

in which a_1, a_2 and a_3 are constants.

1.2.2 Constant normal stiffness

In the following three models, among several, applicable under the CNS boundary condition are presented. Common to them is that loads are calculated based on increments. Leichnitz (1985) proposed the following relations between a shear force increment $dT$and a normal force increment dN from a shear displacement increment $d\delta_{\mathrm{s}}$ and a normal displacement increment $d\delta_{\mathrm{n}}$

$$\begin{bmatrix} dT \\ dN \end{bmatrix} = \begin{bmatrix} k_{\mathrm{s}}^* + \mu^* \cdot \upsilon^* \cdot \kappa^* & \mu^* \cdot \kappa^* \\ \upsilon^* \cdot \kappa^* & \kappa^* \end{bmatrix} \begin{bmatrix} d\delta_{\mathrm{s}} \\ d\delta_{\mathrm{n}} \end{bmatrix}, \tag{13}$$

in which k_{s}^* is the shear stiffness change at constant normal force, μ^* is the change in shear force with normal force at constant shear displacement, υ^* is the angle of dilation at constant shear displacement, and κ^* is the reciprocal of the normal stiffness at constant normal load.

Indraratna et al. (2010) developed the following model predicting τ

$$\tau = \left(\sigma_{\mathrm{n0}} + \frac{k_{\mathrm{n}} \cdot \delta_{\mathrm{n}}}{\tan(\phi_{\mathrm{b}} + \acute{\iota})}\right) \cdot \frac{\tan(\phi_{\mathrm{b}}) + \tan(\acute{\iota}_0)}{1 - \tan(\phi_{\mathrm{b}}) \cdot \tan(\acute{\iota})}, \tag{14}$$

in which δ_{n} is expressed with a Fourier series as

$$\delta_{\mathrm{n}} = \frac{a_0}{2} + \sum_{n=1}^{N_{\delta_{\mathrm{s}}}} L_{\mathrm{f}} \left[a_{\mathrm{n}} \cos \frac{\delta_{\mathrm{s}} 2\pi n}{T} + b_{\mathrm{n}} \sin \frac{\delta_{\mathrm{s}} 2\pi n}{T}\right], \tag{15}$$

where σ_{n0} is the initial normal stress, k_{n} is the normal stiffness, $\acute{\iota}_0$ is the initial asperity angle, a_0, a_{n} and b_{n} are Fourier coefficients, $N_{\delta_{\mathrm{s}}}$ is the number of harmonics, T is the Fourier period, and L_{f} is the Lanczos sigma factor (Weisstein 2008).

The shear behaviour model proposed by Lee et al. (2014) reads

$$\left(\frac{\tau}{\sigma}\right)_{\acute{N}} = 0.017 \cdot JRC^{0.89} \cdot \left(\frac{JCS}{\sigma_{\mathrm{n0}} + \acute{N}j}\right)^{0.42} + \tan(\phi_{\mathrm{b}}), \tag{16}$$

with

$$(\delta_{\mathrm{s}})_{\acute{N}} = \left(\left(\frac{\tau}{\sigma}\right)_{\acute{N}} \Big/ k_{\mathrm{s}} \right) \cdot \left(\sigma_{\mathrm{n0}} + \acute{N}j\right), \tag{17}$$

in which $\acute{N}$ represents the number of steps required to move the next increment, and j is a variable that controls the size of the increment.

1.3 Laboratory direct shear testing equipment

From the presented examples of some theoretical models, it follows that both the development and validation of reliable models require the accurate extraction of loads, stresses, displacements, joint morphology, and apertures from laboratory direct shear testing using rock joint specimens.

The requirements and procedures for performing laboratory direct shear tests are described in Muralha et al. (2014). In this section, an overview of the design principles of direct shear test equipment is provided as background for discussions on uncertainties in Section 1.5. The components in the equipment must have high mechanical strength to withstand the loads and are typically manufactured from steel or cast iron.

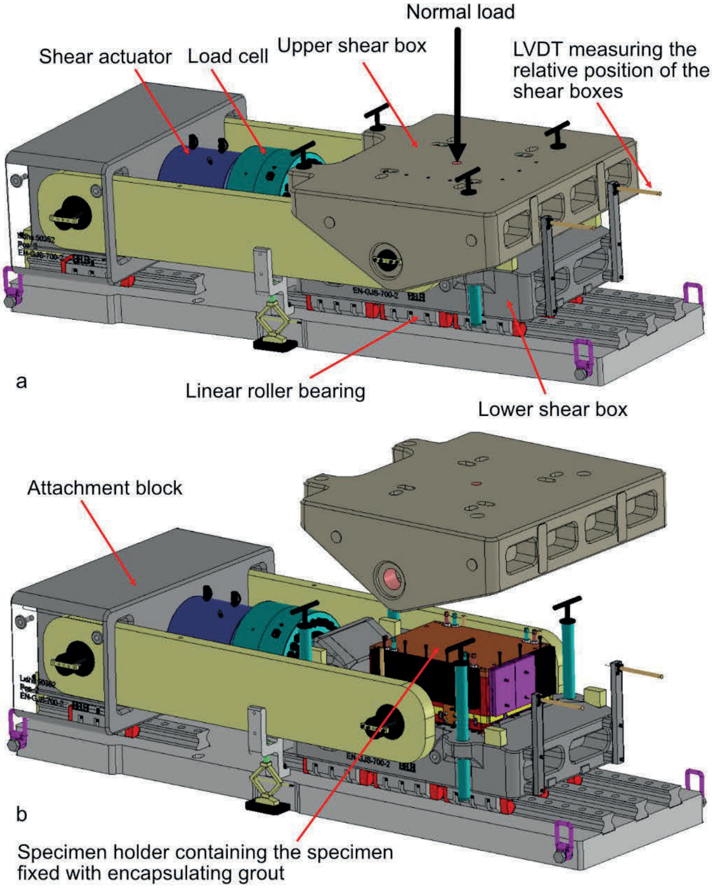

Figure 3. The design principles for a direct shear testing equipment, shown assembled (a) and with the upper shear box separated making the specimen holder visible (b).

With reference to Figure 3, each part of the rock joint specimen is fixed to a specimen holder with encapsulating grout. The specimen holders are, in turn, fixed to the lower and the upper shear boxes, respectively. The shear force is imposed by an actuator via a load cell to the lower shear box, which moves on linear roller bearings, while the upper shear box remains fixed in the horizontal direction, inducing shear movement in the joint. The normal load is applied at the centre of the upper shear box in the same manner as the shear load.

Shearing takes place under a constant shear displacement rate. The shear displacement is measured with a linear variable displacement transformer (LVDT) as the distance between the attachment block and the position of the piston of the shear actuator. This reading serves as the control signal to the control system. The data is collected from the load signals of the actuators and the LVDTs measuring the relative displacement between the shear boxes. Separate LVDTs are used for measuring the shear and normal displacements, respectively.

1.4 Sources of uncertainties

The process of developing models to predict the shear mechanical behaviour of rock joints is illustrated in Figure 4. Samples are extracted from rock joints and prepared for laboratory direct shear testing. The data collected during testing is analysed and forms the background information for both the development and validation of theoretical models. In this section, examples of uncertainties associated with each step are provided, starting with rock joints.

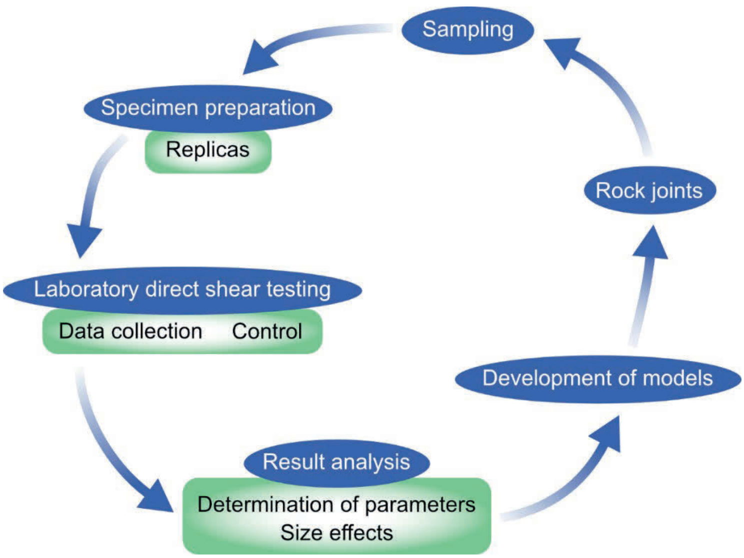

Figure 4. The continuous process of developing and improving models to predict the shear mechanical behaviour of rock joints.

1.4.1 Rock joints

An uncertainty related to rock joints that remains an issue after over four decades of debate is whether and how to account for the influence of the joint size on the shear mechanical behaviour. For technical reasons, rock joint specimen sizes in laboratory direct shear testing are considerably smaller than the size of full-scale rock joints. The influence of joint size on the shear mechanical behaviour of various parameters has been studied by several authors, occasionally yielding contradictory results. The influence of joint size on shear strength has been studied by, e.g., Bandis (1981) and Kutter et al. (1990), on shear stiffness by e.g., Muralha et al. (1990a) and Giwelli et al. (2014), and on dilation angle by e.g., Barton et al. (1977) and Abolfazli et al. (2020).

1.4.2 Sampling

Both the joint morphology and the mechanical properties vary locally. Therefore, methods accounting for variability, e.g., statistical methods should be used when evaluating shear mechanical behaviour, as suggested by e.g., Pinto da Cunha (1991). Despite this fact, with a few exceptions, e.g., Muralha et al. (1990a, b) and Johansson et al. (2010), most studies present results only from a single measurement or mean values for each tested parameter combination. Consequently, the lack of accounting for sample variations constitute an uncertainty.

1.4.3 Specimen preparation

One of several uncertainties related to the specimen preparation procedure is the geometry and strength of the grout encapsulating the specimen and fixing it to the specimen holder. Unless tightly fixed to the specimen holder or specimen, additional shear deformations, beyond those in the joint, will be incorporated into the LVDT measurements. The same would occur normal to the joint if the contact area between the top surface of the grout and the specimen holder is uneven.

The shear strength of a joint, defined as the shear stress at the state of fully mobilized friction, which not necessarily coincides with the peak or maximum shear stress, occurs at small shear displacements, for granite, this is typically about a millimetre, according to LVDT measurements. This makes the joint walls sensitive to their relative positioning during grouting, particularly for natural joints, where the degree of interlocking is limited. Disturbed joints (with respect to the relative position) may yield erroneously measured displacements.

Within science, a commonly used approach is to carry out parametric studies, in which repeated tests are conducted, changing one parameter at a time. However, it is not possible to carry out parametric studies using rock joints, since they are unique by nature (e.g., Grasselli 2001). A way to handle this issue is to conduct multi-stage direct shear testing, i.e., using a single specimen in several tests. However, this practice has several issues related to gradual morphological degradation, as summarized by

MacDonald et al. (2023). Alternatively, replicas of rock joints can be used. For successful utilization of replicas, two important sources of uncertainties need to be controlled, namely, deviations in geometry and mechanical properties between the rock joint as reference and the replicas.

1.4.4 Laboratory direct shear testing

An initial example of uncertainty within laboratory direct shear testing originates from the tensile stresses occurring in the trailing edges. During shearing, such stresses could initiate breakage of the trailing edges, as noted by e.g., Hencher at al. (1993) and Packulak et al. (2018). An example is presented in Figure 5, showing one of the specimens dimensioned 300 mm × 500 mm after direct shear testing. The broken trailing edge of the lower wall is seen to the right, and the broken edge of the upper wall is lying on top of the lower wall to the left. After breakage of the edges, they will not be active as intended in shearing, and the actual joint area is smaller than calculated from the nominal set as input to the control system, which yields errors in the measurements of the stresses.

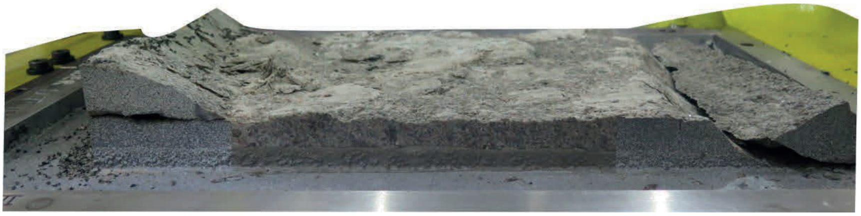

Figure 5: Breakage of trailing edges.

A second example is related to the fact that no test system, i.e., all parts between the measuring points of the LVDTs, is infinitely rigid. Consequently, the measured displacements will be affected by the experimental technique, as recognized by e.g., Rosso (1976) and Bandis (1980). Examples of parts potentially affecting measurements of displacements include irregularities in contact areas and deformations in materials between the locations of the measuring points.

1.4.5 Result analysis

Several sources of uncertainties related to the analyses of results exist. Some examples are provided here. As exemplified in Section 1.2, some theoretical models require measurement of the aperture. Figure 6 shows the trace of a 500 mm long tensile induced rock joint, created by splitting an intact block using sledgehammer and wedges, in unloaded and undisturbed position, i.e., the joint walls have not been separated since the creation of the joint. As can be seen, there is a separation between the joint walls. An uncertainty, therefore, is how to determine the aperture under the normal stress condition specified for the direct shear test.

Figure 6: The trace of a long side of one of the specimens, sized 300 mm × 500 mm, from the experimental program.

Some uncertainties are related to how to determine parameters from the collected data. One of these parameters is the shear strength. Firstly, a physically based definition of shear strength is missing in the literature. Secondly, the appearance of the shear stress versus shear displacement plots varies (Figure 7), and it is not known how to consistently identify the shear strength, as recognized by e.g., Muralha et al. (1990a) and Lee et al. (2014).

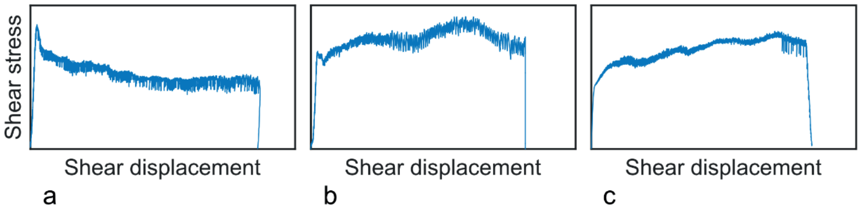

Figure 7: Examples of appearances of shear stress versus shear displacement plots that illustrate the challenge of consistently determining the shear strength.

The shear stiffness is a second parameter that also lacks a physically based definition and a consistent approach for determination, as acknowledged by e.g., Kulatilake et al. 2016 and Day et al. (2017). Figure 8 shows examples of plots of shear stress versus the initial 1.5 mm of shear displacement, which illustrate the challenge of consistently determining the shear stiffness.

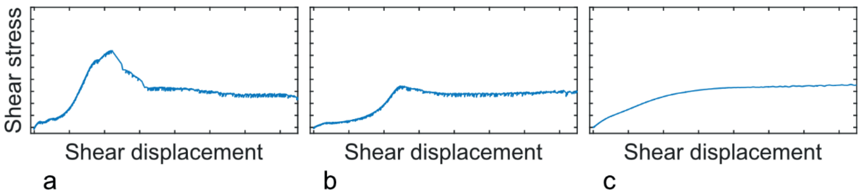

Figure 8: Examples of appearances of shear stress versus shear displacement plots for the initial 1.5 mm of shearing, illustrating the challenge of consistently determining the shear stiffness.

A way to address the fact that no test system is infinitely rigid is to conduct a test using a low-deformability dummy specimen, such as steel, and correct for the influence of the deformations in the test system by subtracting the displacements in the dummy test from the displacements in rock joint tests (see e.g., Chryssanthakis 2004 and Muralha et al. 2014). Since the displacements measured in the dummy test are of the same order as those measured in the rock joint direct shear test, the differences are very small and sensitive to variations. This is illustrated in Figure 9, which shows parts of the fourth cycle in normal loading tests (coloured) with dashed lines representing the secant normal stiffnesses. The corresponding curves, after subtraction of displacements from the dummy test, are shown in black, along with the recalculated secant normal stiffnesses. Firstly, it is noted that there is clearly a need to compensate for the influence of displacements originating from imperfections in the test system. Secondly, the magnitude of the displacements after compensation, reflecting the deformations in the joint, is very small, on the order of hundreds of millimetres, demonstrating a high sensitivity to variations, which occasionally results in erroneous negative normal stiffnesses.

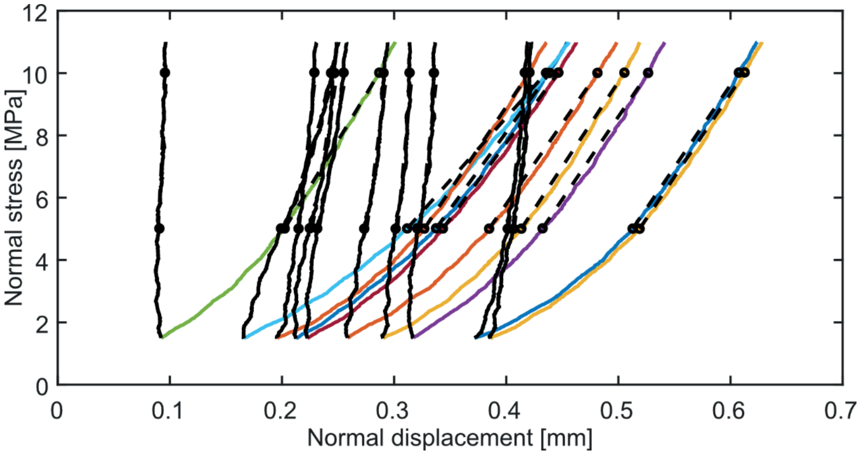

Figure 9: Examples of normal stiffnesses measured from normal loading tests (coloured), and after compensation using a dummy test with a steel specimen (in black).

1.4.6 Development of models

There are several shear mechanical aspects of interest to describe in relation to the derivation and validation of theoretical models. In this section, some observations made during the research are presented as illustrative examples of open issues related to the derivation and validation of theoretical models. In Section 1.2, examples of models predicting peak shear strength and shear stiffness are presented. Other parameters of relevance to predict are the residual shear strength (e.g., Casagrande et al. 2018) and the residual dilation angle (e.g., Zhao et al. 2022). One suggested theory of plasticity is that first the steepest asperities are subjected to stress concentrations until failure, which, after stress redistribution, is followed by contact of gradually less steep asperities (e.g., Kutter et al. 1990 and Grasselli et al. 2002). Figure 10 shows the range of the sizes of material, from grain size to several centimetres, separated from a joint sized 300 mm × 500 mm after about 20 mm of shear displacement. The regularly observed non-linearity preceding the state of fully mobilized friction, regardless of if there is a clearly distinguishable peak shear stress, e.g., Figure 8a and b, or a continuous non-linear appearance, e.g., Figure 8c, indicates that plasticity occurs through gradual breakage of asperities. This statement, combined with the fact that not only asperities are coming loose, but also that parts of the surfaces of some of the largest pieces have been subjected to wear before coming loose (Figure 10), suggests that the theory of breakage of gradually less steep asperities may not be applicable throughout the residual shear stress state. Instead, in the residual shear stress state, stresses causing breakage through larger volumes appear to interact with stresses causing breakage at the asperity level. From Figure 10, there is also uncertainty about the meaning of “gradual” and “asperity”.

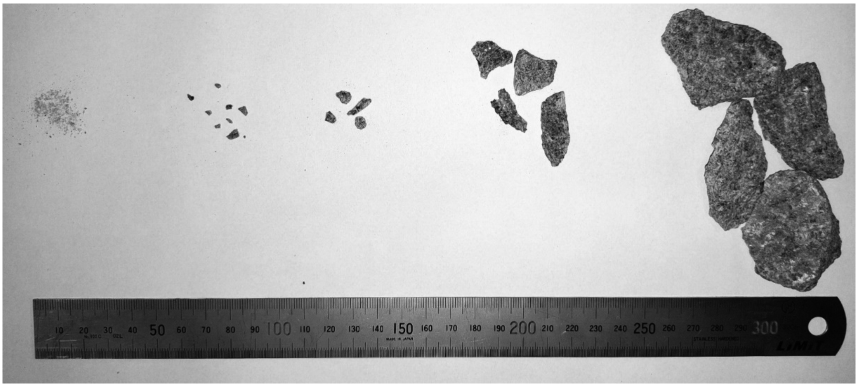

Figure 10: Photograph illustrating the variety of fragment sizes that detached during approximately 20 mm of shearing in a 300 mm × 500 mm rock joint specimen tested in the experimental program, with the ruler included for scale.

The joint morphology has been described in various terms. Bandis et al. (1981) divided roughness into a geometrical component and an asperity component. Huang et al. (2020) used the term waviness. Undulation and amplitude of undulation were used by Leal-Gomes (2003) to characterize joint morphology. Figure 11 shows the shear stress versus shear displacement plots from direct shear testing under the CNL boundary condition for three high-strength concrete replicas. For these specimens, the geometrical deviations of the lower parts relative to a reference surface, derived from 3D scans before direct shear testing, are shown in Figure 12. Specimen 1, which has the highest peak shear strength and residual shear strength, has a geometry similar to that of specimen 3. Specimen 3 has shear strength and residual shear stress similar to that of specimen 2, which, in turn, has a smaller circular depression and smaller deviations along the edges compared to specimen 1 and specimen 3. The replicas were casted from moulds with identical roughness (features of short wavelengths in the order of tenths of millimetres). Figure 13 shows surface comparisons of 3D scans between the lower and upper parts before direct shear testing. As expected, it is observed that the joint matching is complete and essentially identical among the specimens. Consequently, the discrepancies in the results shown in Figure 11 cannot be explained by differences in joint matching or roughness.

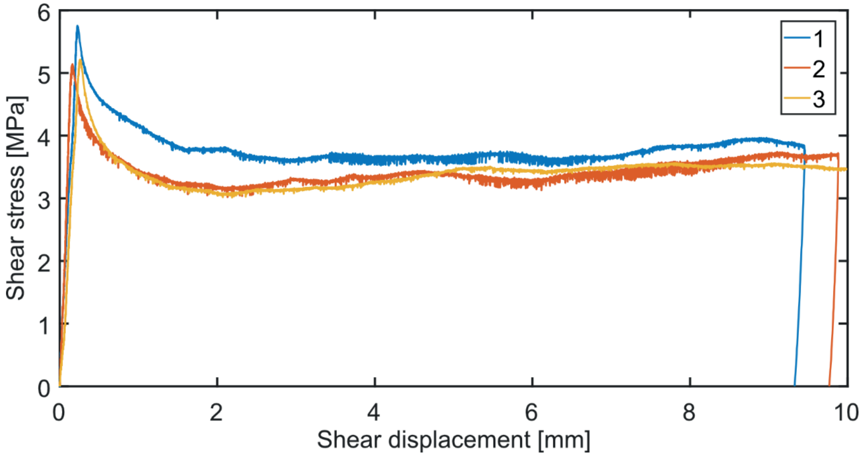

Figure 11: The shear stress versus shear displacement plots from CNL direct shear testing of three high-strength concrete replicas (the unloading cycle of specimen 3 is missing).

The identical joint matching is reflected in the essentially identical wear shown in Figure 14, derived from surface comparisons of 3D scans before and after direct shear testing, and from photos. It can therefore be presumed that the differences in shear mechanical behaviour originate from long-wavelength features (waviness) superimposed onto the roughness. There is uncertainty about how to incorporate the effect of waviness on shear mechanical behaviour in theoretical models.

An additional uncertainty in modelling shear mechanical behaviour in the residual shear strength state, under normal stresses where crushing is the mode predominant over sliding, is how to handle the fact that surfaces initially in contact are not necessarily active during shearing, and vice versa. This is exemplified in Figure 15a, which shows the areas in initial contact in a rock joint specimen sized 300 mm × 500 mm, and the photo in Figure 15b, showing the wear after about 50 mm of shearing, and in Figure 15c showing the wear derived from surface comparisons of 3D scans before and after shearing.

Finally, generally, most laboratory direct shear tests have been carried out under normal loads lower than 2 MPa, and the number of results from experimental studies under the CNS boundary condition is limited. Additionally, with a few exceptions (e.g., Yoshinaka et al. 1991 and Uotinen et al. 2021), the joint sizes used in direct shear testing have been less than about 400 cm^2. Overall, the limitations in data range constitute an uncertainty in the generalization of theoretical models.

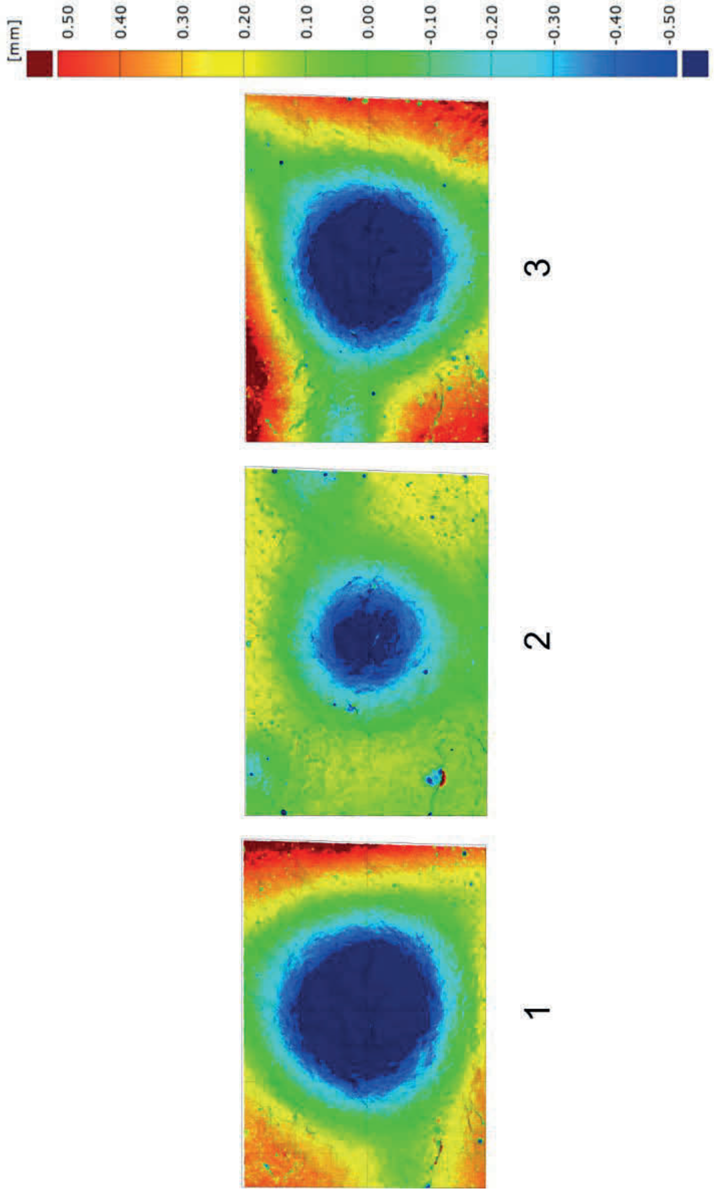

Figure 12: Surface comparisons of the specimens tested in Figure 11, showing the deviations relative to a reference surface before direct shear testing.

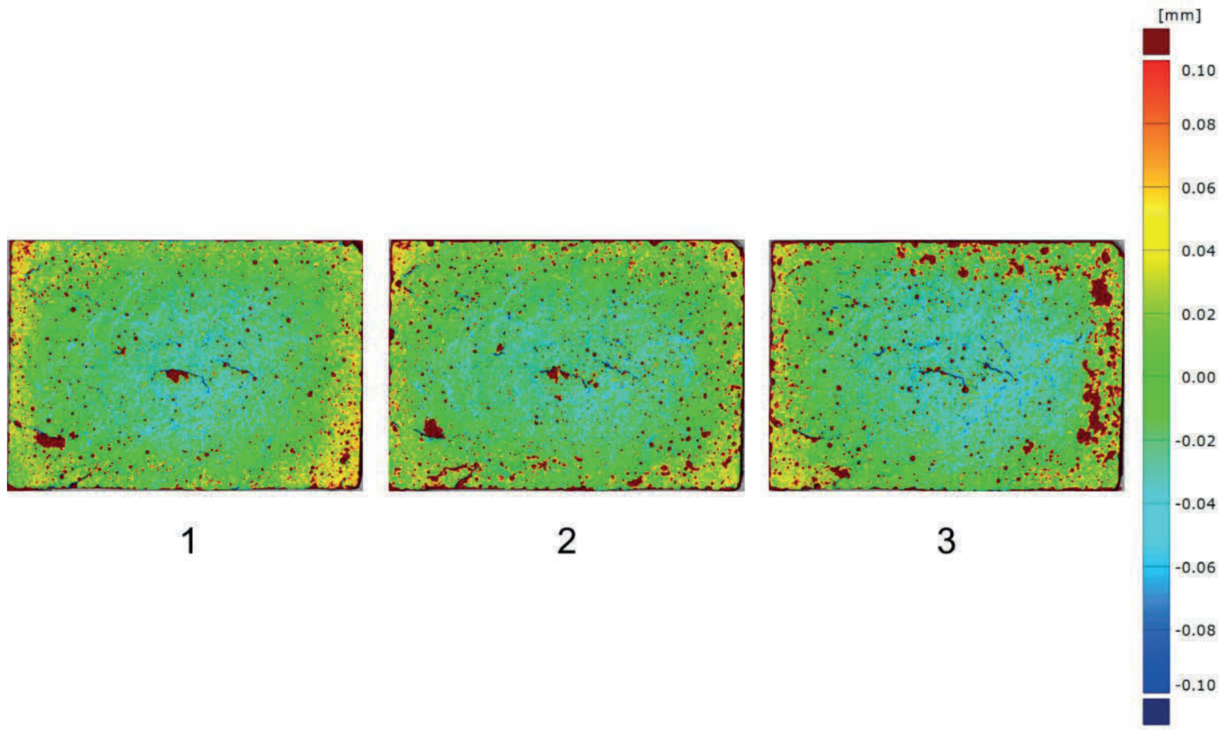

Figure 13: Surface comparisons between the lower and the upper specimens of the specimens tested in Figure 11, showing that the joint matching is complete and essential identical.

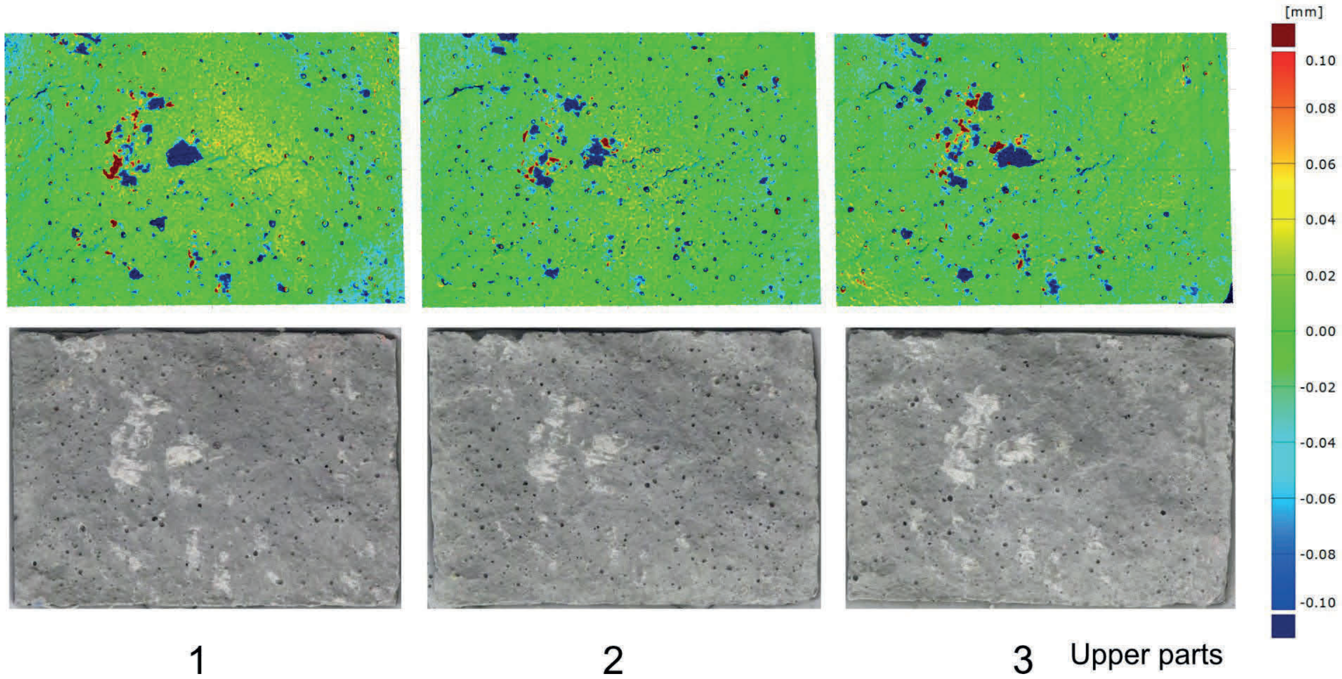

Figure 14 (upper parts): The essentially identical wear, shown in blue, evaluated from surface comparisons of 3D scans before and after direct shear testing of the specimens tested in Figure 11, and from photos (greyscale with wear in white).

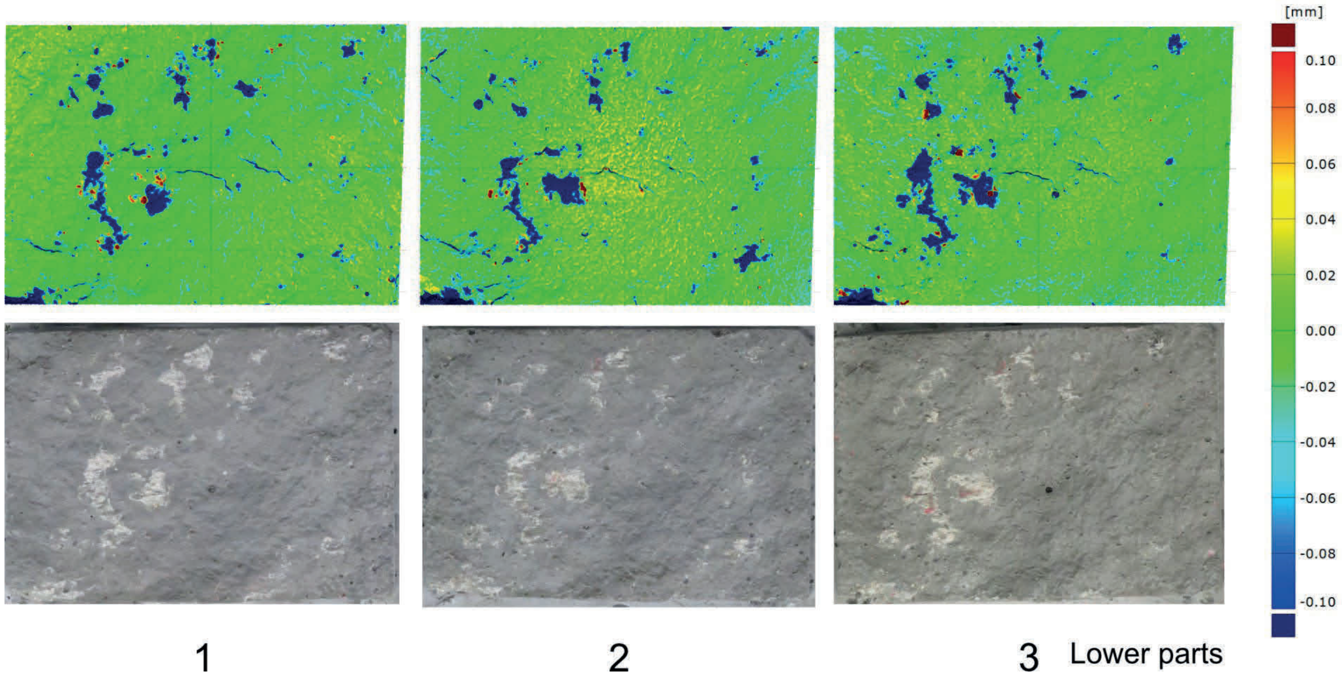

Figure 14 (lower parts): The essentially identical wear, shown in blue, evaluated from surface comparisons of 3D scans before and after direct shear testing of the specimens tested in Figure 11, and from photos (greyscale with wear in white).

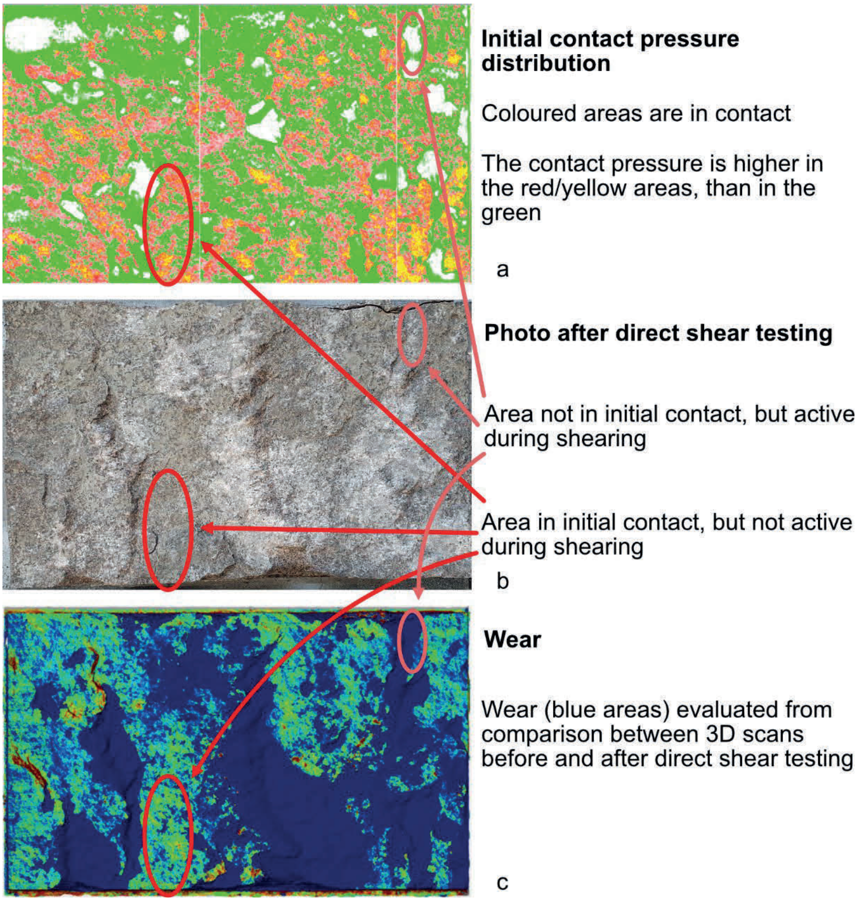

Figure 15: The areas in contact before direct shear testing in a rock joint specimen sized 300 mm × 500 mm (a), a photo of the specimen after direct shear testing showing the wear areas in light grey (b), and the wear evaluated from comparison between 3D scans, with areas subjected to wear in blue (c).

1.5 Objectives

The overall objective of the work herein presented is to facilitate development of improved criteria for prediction of shear strength of rock joints. This will allow for cost reductions, more efficient usage of underground space, reduced environmental impact, and better control of safety margins of structures founded on or excavated in rock.

The work presented in this report supports the overall objective by analysing the data set from the experimental project, aiming to provide novel approaches and methods that yield improved accuracy in direct shear testing of rock joints and in the evaluation of the results. Improved accuracy of the parameters derived from direct shear testing results is, in turn, a prerequisite for improved shear strength criteria.

Specifically, the following research questions are addressed:

RQ 1: How can uncertainties in the results from direct shear testing of replicas, which originate from geometrical deviations between the rock and replica fracture surfaces, be minimized?

RQ 2: How can errors in the applied normal load during direct shear testing under the CNS boundary condition, which originate from imperfections in the test system, be minimized?

RQ 3: How can uncertainties in studying the shear strength and shear stiffness of rock joints from laboratory direct shear testing, which originate from the lack of consistent definitions and approaches for measuring these parameters according to the definitions, be minimized?

RQ 4: What are the errors in measuring shear stiffness that originate from the incorporation of unavoidable deformations in the test system during conventional indirect displacement measurements, and how can displacements be measured directly over the joint?

RQ 5: How can uncertainties in evaluating the influence of the specimen size on the shear strength and shear stiffness be reduced, and is there an influence of joint size on these parameters?

1.6 Limitations

The experimental study, from which the results are based, is limited to joint areas between 21 cm^2 and 1500 cm^2, one initial normal stress of 5 MPa, one constant shear displacement rate of 0.5 mm/min and one material, granite, extracted from one quarry. The natural joints had a small amount of infill material (calcite) and limited weathering. The direct shear tests were carried out in two different setups and one type of replicas was tested. The general applicability of the results, therefore, needs to be verified by replicating the original experiments through independent studies using other materials and direct shear test setups. Interaction between fractures in a network and hydromechanical aspects have not been investigated.

2. MATERIALS AND METHODS

Section 2.1 to Section 2.6 provides an overview of the materials and methods used in the experiments. The research methodology, presented in Section 2.7, describes how the research questions introduced in Section 1.5 were addressed and analysed using the materials and methods.

2.1 Materials

Two granite blocks with a weight of 15 and 20 metric tons, respectively, were extracted from the Flivik quarry in Sweden. The granite is medium grain sized and belongs to the TIB-1 (Transscandinavian Igneous Belt) suite of plutonic rocks emplaced in the period 1.81-1.76 billion years ago (Högdahl et al. 2004). Forty-six specimens distributed over three sizes were manufactured: 35 mm × 60 mm, 70 mm × 100 mm and 300 mm × 500 mm. The specimens were of two types: undisturbed natural, with small amount of infill material (calcite) and limited weathering; and artificially tensile induced (fresh and well-mated), created using a sledgehammer and wedges. The specimens were fixed to the specimen holders with encapsulating grout of the UHPC (Ultra High Performance Cementitious) Ducorit®S5 from ITW Performance Polymers.

Fifteen replicas were manufactured based on one of the rock joint specimens sized 70 mm × 100 mm, cast in the UHPC Ducorit®D4 from Densit AS from silicone moulds made of ELASTOSIL® M4601 A/B from Wacker Chemie AG containing imprints of the joint surfaces. These replicas were used for geometrical evaluations. In addition, six of the replicas were subjected to direct shear testing and evaluated against the shear mechanical behaviour of the rock joint.

The naming nomenclature of the rock joint specimens are *Joint typeNumber-Size-Boundary condition*. *Joint type* is either natural (N) or tensile induced (TI). *Number* is an identification number. *Size* refers to the joint size and is either S, M or L, corresponding to the sizes 35 mm × 60 mm, 70 mm × 100 mm and 300 mm × 500 mm, respectively. *Boundary condition* is either CNL or CNS. For example, N1-S-CNS is a natural specimen with identification number 1, sized 35 mm × 60 mm, and tested under the CNS boundary condition.

The naming nomenclature of the replica rock joint specimens are *RMatching-N1-Boundary condition(Part)Number*. *R* indicates that the specimen is a replica. *Matching* is either "NM" or "PM", referring to natural match or perfect match, respectively. A natural match means that both surfaces of the rock joint were replicated. A perfect match means that only the lower part of the rock joint was replicated, with the upper part of the replica was made as a negative cast of the lower. *N1* refers to the designation of the rock joint the replicas were manufactured from. When needed for clarity, *Part* is included in the replica name and is either "L" or "U", corresponding to the lower or upper parts, respectively. *Number* is an identification number. For example, RNM-N1-CNL-6L is the lower part of a naturally matched replica with identification number 6, tested under the CNL boundary condition.

2.2 3D scanning

All joint surfaces were 3D scanned before and after direct shear testing to facilitate quantitative analyses of areas in contact and wear. Depending on specimen size, two 3D scanning techniques were used.

A blue LED structured light technology was employed to the specimens sized 35 mm × 60 mm and 70 mm × 100 mm using a hand-held Artec Spider scanner from Artec 3D with the post-processing accomplished in the software Artec Studio, versions 2011 – 2013.

A 3D laser scanning technique consisting of a hand-held Leica Absolute Scanner with a Leica Absolute Tracker AT960 was employed to the specimens sized 300 mm × 500 mm. The post-processing of the point clouds was accomplished in SpatialAnalyzer® and in Leica Cyclone 3DR.

The point clouds were converted to surface models in STL (stereolithography) format, composed of triangular planes, for subsequent surface comparisons and wear evaluations.

2.3 Contact pressure measurements

The contact pressure distributions of the rock joints were documented before direct shear testing using the Fujifilm pressure measurement film Prescale of type LW. Subjecting the pressure sensitive film to a normal stress, areas in contact became red with the colour intensity corresponding to a certain pressure value. Then, the colourized film was digitized using a dedicated scanner and software from the Fuji Digital Analysis System of model FDP-8010E.

2.4 Surface comparison

A surface comparison is the operation of calculating and visualizing the differences between the coordinate points in two STL surface models. Such operations were accomplished in commercially available software GOM Inspect (2018).

2.5 Laboratory direct shear testing

The specimens sized 35 mm × 60 mm and 70 mm × 100 mm were tested in a 300 kN GCTS direct shear testing equipment. The specimens sized 300 mm × 500 mm were tested in a direct shear testing equipment developed at RISE Research Institutes of Sweden according to the design principles described in Section 1.3, with a 5 MN capacity for both normal and shear loading. In shear testing, the equipment was mounted in a 20 MN load frame, from which the normal load was applied (see Figure 3 and Figure 16). The tests were, in addition to the CNL boundary condition, conducted under the CNS boundary condition at a constant and initial normal stress of 5 MPa, respectively. The displacements were measured both conventionally with linear variable displacement transformers (LVDTs), indirectly through the relative position of the shear boxes, and directly over the traces of the joints, using optical digital image correlation (DIC).

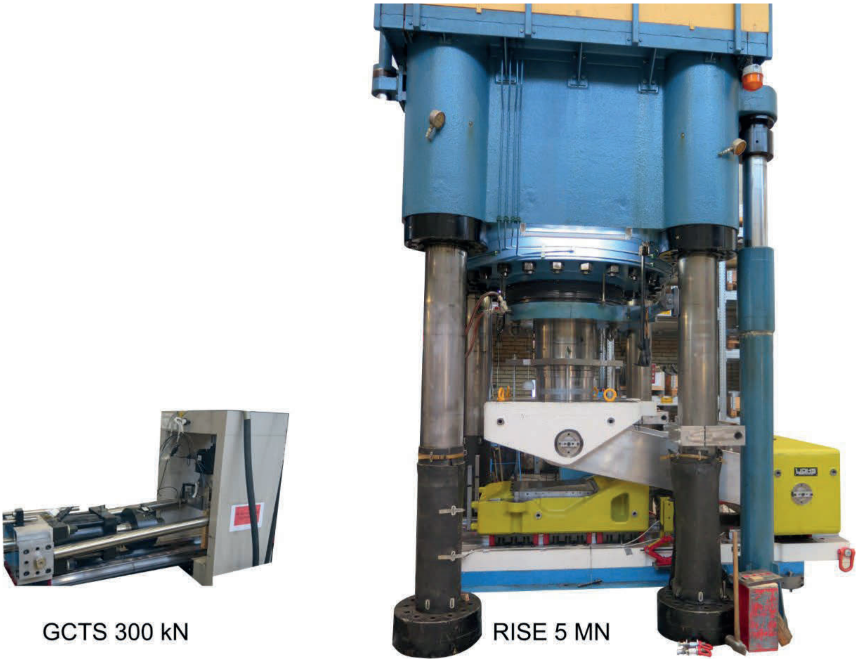

Figure 16: Photos of the equipment used for direct shear testing illustrating the proportions.

2.6 Analysis of variance

Analysis of variance (ANOVA) is an established statistical technique for making statistical inferences from several means, see e.g., Johnson (2018). By applying ANOVA to a data set, statistical inferences on the effects from various factors on a response variable (i.e., the variable being investigated) can be made. For each factor, it can be concluded, at a certain level of significance, whether it has an impact on the response variable. If it does, the effect of the factor can be quantitatively estimated. The effect on the response variable from various factors is investigated by calculating the sum of the squares of the differences between the means of the factors and the grand total mean. This sum then is divided by the degrees of freedom to obtain the mean squares of the factor effects. The error sum of squares, estimating the random error, is calculated by summing the squares of the differences between the individual observations and their group means, followed by dividing by the degrees of freedom. The test statistics is an F test on the ratio of the mean square of the factor effect to the error sum of squares. A large ratio indicates an impact of the factor on the response variable. The statistical analyses were performed in the software SPSS (2023).

2.7 Research methodology

Figure 17 illustrates the workflow. The work began by investigating the differences in shear mechanical behaviour between a set of replicas and the rock joint from which they were made and analysing these differences with respect to geometrical deviations. Consequently, this study addresses RQ 1 (reduction of uncertainties in the results from direct shear testing of replicas, originating from geometrical deviations between the rock and replica fracture surfaces). The rock joint and the replicas were manufactured from the materials presented in Section 2.1. Before and after direct shear testing the joint surfaces where 3D scanned. An introductory analysis is presented in Larsson et al. (2020a). By conducting surface comparisons between replicas and the rock joint along with analyses of contact pressure distributions, errors in the replica manufacturing process were studied, and geometrical deviations between the replicas and the rock joint visualized and explained. In Larsson et al. (2023a), the analyses are elaborated and expanded. Two geometrical quality parameters were developed and the ability to geometrically reproduce replicas within narrow tolerances was studied. In Larsson et al. (2023b), the geometrical quality assurance parameters are validated and the mechanical replicability of geometrically quality assured replicas demonstrated.

The subsequent parts of the work included direct shear testing under the CNS boundary condition. As a measure to generate accurate shear test data, the issue of error in the applied normal load during direct shear testing under the CNS boundary condition, originating from imperfections in the test system, was first addressed (RQ 2). In Larsson et al. (2020b), an approach to compensate for this type of error is presented. The approach was validated in the GCTS direct shear test equipment, in which the specimens sized 35 mm × 60 mm, and 70 mm × 100 mm were tested. The result from the application of the approach is unique to the direct shear test setup in question. Therefore, as a part of the commissioning of the shear test equipment developed at RISE and as a prerequisite to subsequent direct shear testing of specimens sized 300 mm × 500 mm, the approach was applied to the setup with the 5 MN shear test equipment mounted to the 20 MN normal loading frame (Larsson 2021).

Having taken all the preparatory measures, next, the extensive test program was executed, allowing for handling the uncertainties associated with previous studies and expanding the existing range of knowledge. This was achieved by testing several samples for each parameter combination of different joint types under different boundary conditions, under previously unexplored combinations of stresses occurring at depths of several hundreds of meters and a wide range of joint sizes. With access to the resulting data set, one of the research questions of fundamental interest was to investigate the influence of specimen size on shear strength (RQ 5). Before doing so, the uncertainties originating from the lack of a consistent definition of shear strength needed to be addressed (RQ 3). In Larsson et

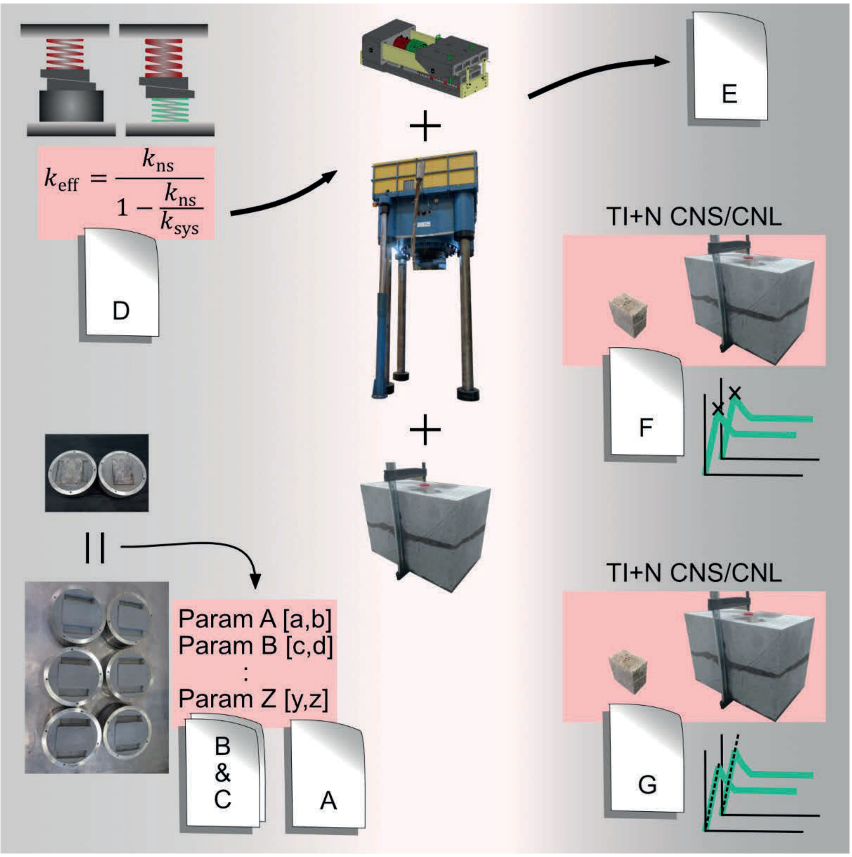

Figure 17: Illustration of workflow and the relation between Larsson et al. (2020a) (A), Larsson et al (2023a) (B), Larsson et al (2023b) (C), Larsson et al. (2020b) (D), Larsson (2021) (E), Larsson et al. (2025a) (F) and Larsson et al. (2025b) (G).

al. (2025a), first, a consistent definition, along with an approach for determining shear strength according to this definition, is presented. Then, the uncertainty related to the influence of specimen size on shear strength is handled by applying ANOVA to the data set with shear strength as the response variable.

A second parameter of fundamental interest to investigate is the shear stiffness (Larsson et al 2025b. Following the workflow in Larsson et al. (2025a), first a consistent definition, along with an approach for determining shear stiffness according to this definition, is presented (RQ 3). Then, the uncertainties related to the influence of the stiffness of the test system on the displacements, measured conventionally indirect with LVDTs as the relative displacement between the shear boxes, are investigated by comparisons with direct DIC measurements (RQ 4). Finally, the uncertainty related to the influence of specimen size on shear stiffness is addressed by applying ANOVA to the dataset, with shear stiffness as the response variable (RQ 5).

3. RESULTS

This section summarizes the results of the study and follows the workflow in Figure 17, starting with the results from the analyses of geometrical quality assurance of rock joint replicas in Section 3.1. This is followed by the results from analyses on how to compensate for the influence of the system normal stiffness under the CNS boundary condition in Section 3.2, determination of shear strength and the effect of specimen size in Section 3.3 and finally, determination of shear stiffness and the effect of direct displacement measurement in Section 3.4.

3.1 Geometric quality assurance of rock joints

One fundamental challenge within rock mechanical research is that, unlike many other disciplines, rock joint specimens are inherently unique. This uniqueness prevents structured parametric studies to investigate the influence of different input parameters on a response variable. Tests on rock joint replicas allow us to execute parametric studies, but the outcomes from such studies could be questioned. The shear mechanical behaviour of both the rock joint and the replicas is rarely presented, which means that the accuracy of the results is unknown. In addition, typically, only one replica specimen per parameter setting is tested, as seen in studies by Jing et al. (1992) and Koyama et al. (2008), among others, leaving also the precision of the results unknown. Consequently, it is not possible to determine if the differences between two results is due to random errors or differences in test conditions. Lacking a method to acquire knowledge about the ability of the replicas to imitate the shear mechanical behaviour of the rock joint and their statistical dispersion, an experimental study was conducted. Replicas from a granite rock joint sized 70 mm × 100 mm were manufactured and subsequently direct shear tested along with the rock joint specimen, aiming to derive such method.

The introductory results are presented in Larsson et al. (2020). From surface comparisons of 3D scanned joint surfaces between the rock joint and the replicas geometrical deviations were analysed. Three types of deviations originating from the manufacturing process of the replicas were revealed: pores, deviations originating from positioning of the mould and fragments coming loose from the rock joint in the mould manufacturing process. It was also demonstrated that these sources of errors could be eliminated by improvement of the replica manufacturing process.

Larsson et al. (2023a) deals with geometric reproducibility, i.e., the ability to produce replicas with similar geometries both mutually and in relation to the rock joint from which the replicas were manufactured. Two possible types of geometrical deviations were studied: morphological deviations and deviations with respect to orientation relative to the shear direction. Morphological deviations refer to geometrical differences between the joint surfaces. Deviations with respect to shear direction refer to the event when the orientation of the joint surfaces with reference to the specimen holder (which is parallel to the shear direction) differs. Parameters that capture these types of deviations between the replica and the rock joint were presented. σ_{mf} captures morphological deviations and is calculated as

$$\sigma_{\mathrm{mf}} = \sqrt{\frac{1}{N}\sum_{\mathrm{i}=1}^{N}(\zeta_{\mathrm{i}} - \bar{\zeta})^2}, \tag{18}$$

where N is the number of coordinate points, ζ_{i} is the deviation value along the evaluation direction for the i:th coordinate point, and $\bar{\zeta}$ is the mean of the deviations along the evaluation direction. σ_{mf} is calculated after alignment of the 3D scanning data of the replica with the rock joint. Figure 18 shows σ_{mf} for some replica joint surfaces, demonstrating the correlation with the visualization of deviations derived from surface comparisons between the replica and the rock joint.

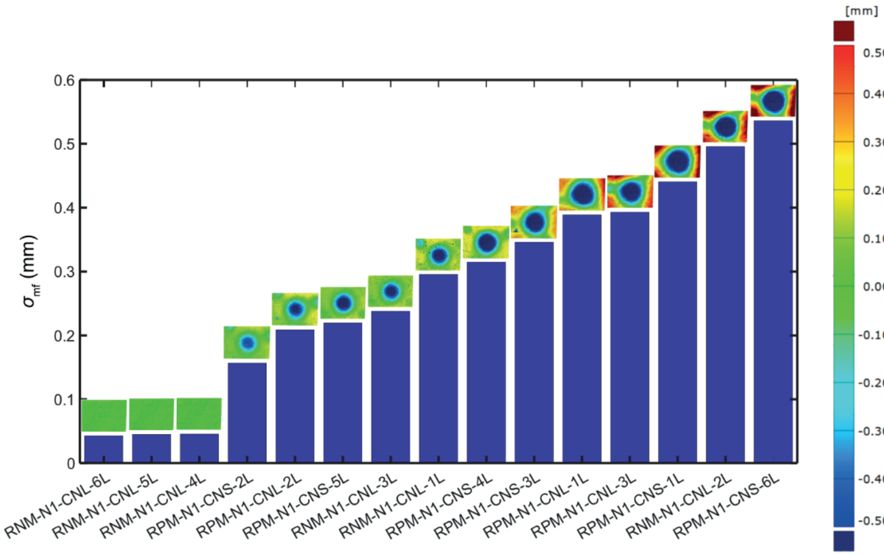

Figure 18: σ_{mf} for some replica joint surfaces, demonstrating the correlation with the visualization of deviations derived from surface comparisons (Larsson et al. 2023a).

The second type of deviation, orientation with respect to shear direction, can after alignment, with reference to Figure 19, be captured by projecting the normal vector, $\boldsymbol{V}$, of the best-fit plane of the replica joint surface, Π, onto the corresponding plane of the rock joint surface, Π_{RP}, denoted $\boldsymbol{V}_2$.This vector contains information about the deviation both in terms of magnitude and direction, is calculated as

$$\boldsymbol{V}_2 = \boldsymbol{V} - \boldsymbol{V}_1 = \boldsymbol{V} - \frac{\boldsymbol{V}\cdot\boldsymbol{V}_{\mathrm{RP}}}{|\boldsymbol{V}_{\mathrm{RP}}|^2}\boldsymbol{V}_{\mathrm{RP}}. \tag{19}$$

Depending on the alignment between the replica and the rock joint, $\boldsymbol{V}_2$ will contain deviations in terms of morphology and orientation, or only morphology. After subtracting the vectors of both alignments, the resulting vector contains only deviations with respect to orientation. By choosing the length of $\boldsymbol{V}$ and $\boldsymbol{V}_{\mathrm{RP}}$ to be 100 mm, this vector is denoted $\boldsymbol{V}_{\mathrm{Hp100}}$, where the subscript refers to the specimen holder position being parallel with the shear direction. Figure 20a shows an example of $\boldsymbol{V}_{\mathrm{Hp100}}$, and Figure 20b shows the corresponding surface comparisons containing deviations in morphology and orientation, and only orientation, respectively. This demonstrates the capability of $\boldsymbol{V}_{\mathrm{Hp100}}$ to capture deviations with respect to orientation.

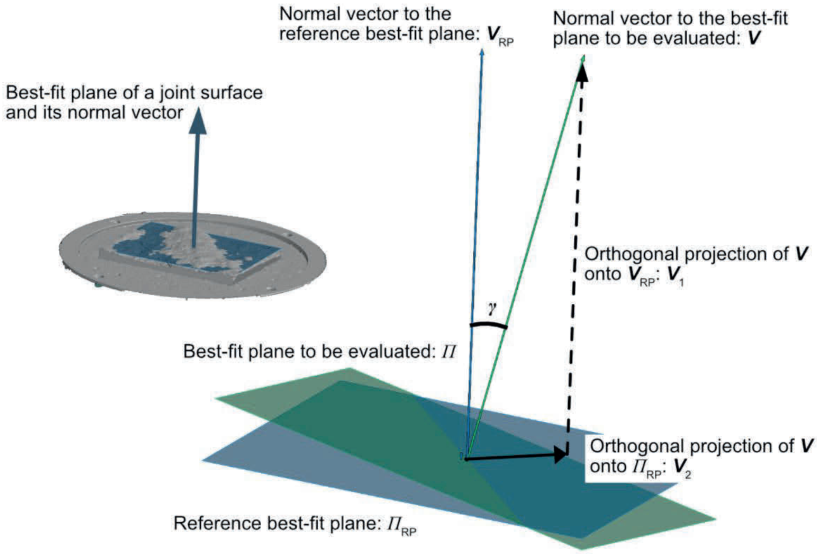

Figure 19: Illustration the vector $\boldsymbol{V}_2$ capturing deviations in orientation with respect to the shear direction (Larsson et al. 2023a).

The mechanical replicability, i.e., the impact of geometrical variation of replicas on shear mechanical behaviour and the difference in shear mechanical behaviour between replicas and rock joint is studied in Larsson et al. (2023b). σ_{mf} and $\boldsymbol{V}_{\mathrm{Hp100}}$ were validated by demonstrating a correlation with the shear mechanical behaviour, explained by the parameters capturing differences in aperture distribution. Two of the replica specimens, designated RNM-N1-CNL-5 and RNM-N1-CNL-6, exhibited essentially identical shear behaviour, thereby demonstrating the possibility of reproducing replicas with high precision. This makes replicas useful in parametric studies. For the specific replica manufacturing process employed in this study, $|\boldsymbol{V}_{\mathrm{Hp100}}|$ equal to 0.2 mm was the largest measured deviation with respect to orientation, which was shown to be of no importance to the shear mechanical behaviour. A threshold value of σ_{mf} less than 0.06 mm was established to ensure the geometry required for reproduction.

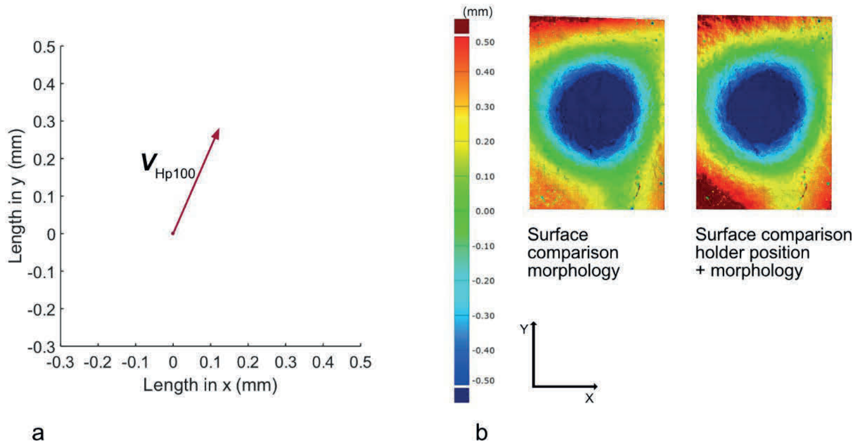

Figure 20: An example of $\boldsymbol{V_{Hp100}}$ (a) and the corresponding surface comparisons (b) (Larsson et al. 2023a).

In summary, in Larsson et al. (2023a), the geometrical quality assurance parameters σ_{mf} and $\boldsymbol{V}_{\mathrm{Hp100}}$, are derived, and their ability to capture geometrical reproducibility demonstrated. In Larsson et al. (2023b), the parameters are validated and the accurate mechanical replicability of geometrically quality assured replicas demonstrated. After these preparatory steps, a method for geometrical quality assurance is presented in Larsson et al. (2023b). The parameters σ_{mf} and $\boldsymbol{V}_{\mathrm{Hp100}}$ are calculated from 3D scans as described in the foregoing. If it is the first time the replica material is used at least five replicas should be direct shear tested along with the rock joint. If the shear mechanical behaviour of the replicas does not replicate the behaviour of the rock joint the replica manufacturing process needs to be changed. On the other hand, if the shear mechanical behaviour of the rock joint is replicated, then threshold values of σ_{mf} and $\boldsymbol{V}_{\mathrm{Hp100}}$ are established from the observed variation. Knowing the threshold values, σ_{mf} and $\boldsymbol{V}_{\mathrm{Hp100}}$ are calculated for each replica before direct shear testing. Only replicas with values lower than the threshold values are qualified for direct shear testing. In this manner, geometrically quality assured replicas could be successfully used in parameter studies offering replicas that imitate the shear mechanical behaviour of the rock joint with known deviation and controlled variation.

This section ends with some observations, made during the development of the geometrical quality assurance parameters, of interest to note. The high geometrical precision of the replicas is reflected in the essentially identical wear shown in Figure 21, which, for comparison, also shows the wear in the rock joint. It is interesting to note that

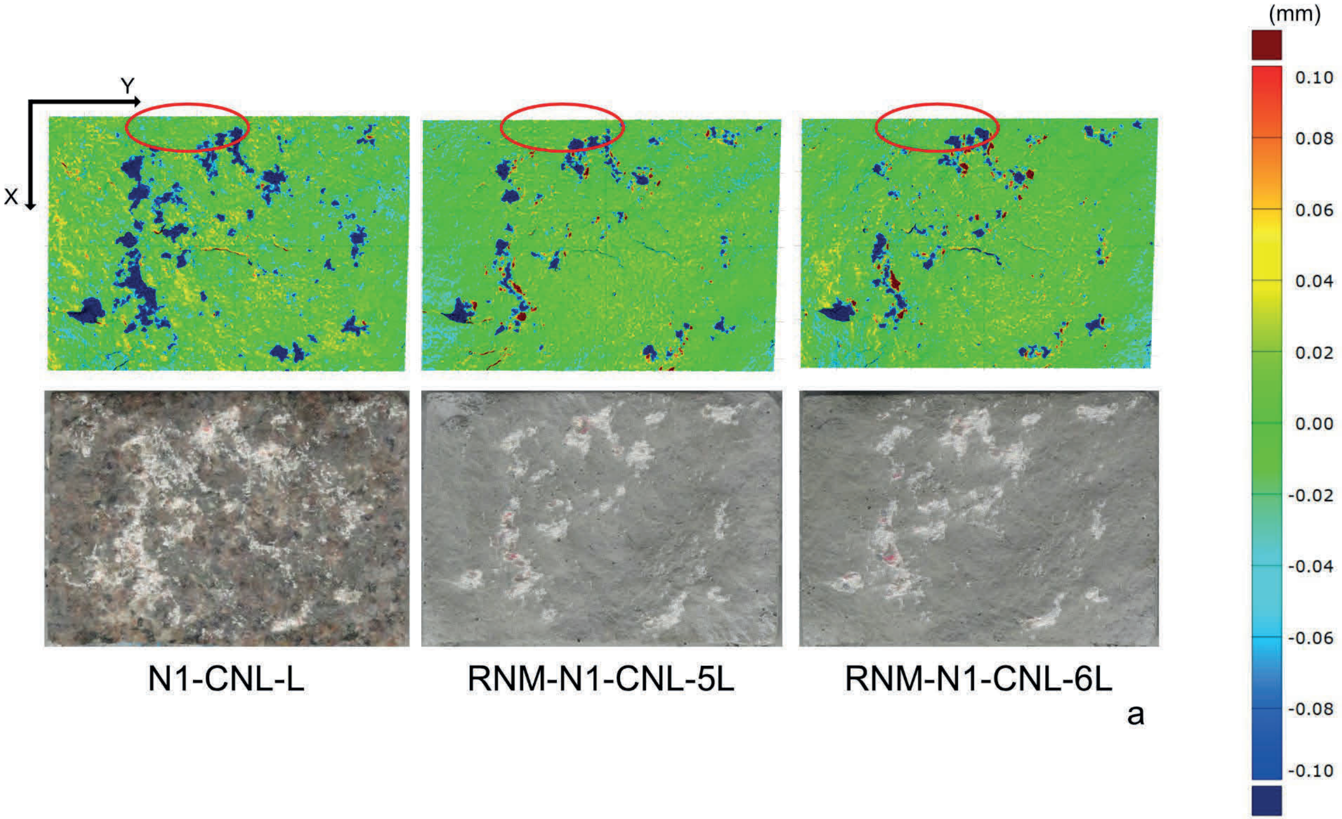

Figure 21 (lower parts): The wear evaluated from surface comparisons of the joint surfaces before and after testing, and photos of (a) the lower parts and (b) the upper parts (Larsson et al. 2023b).

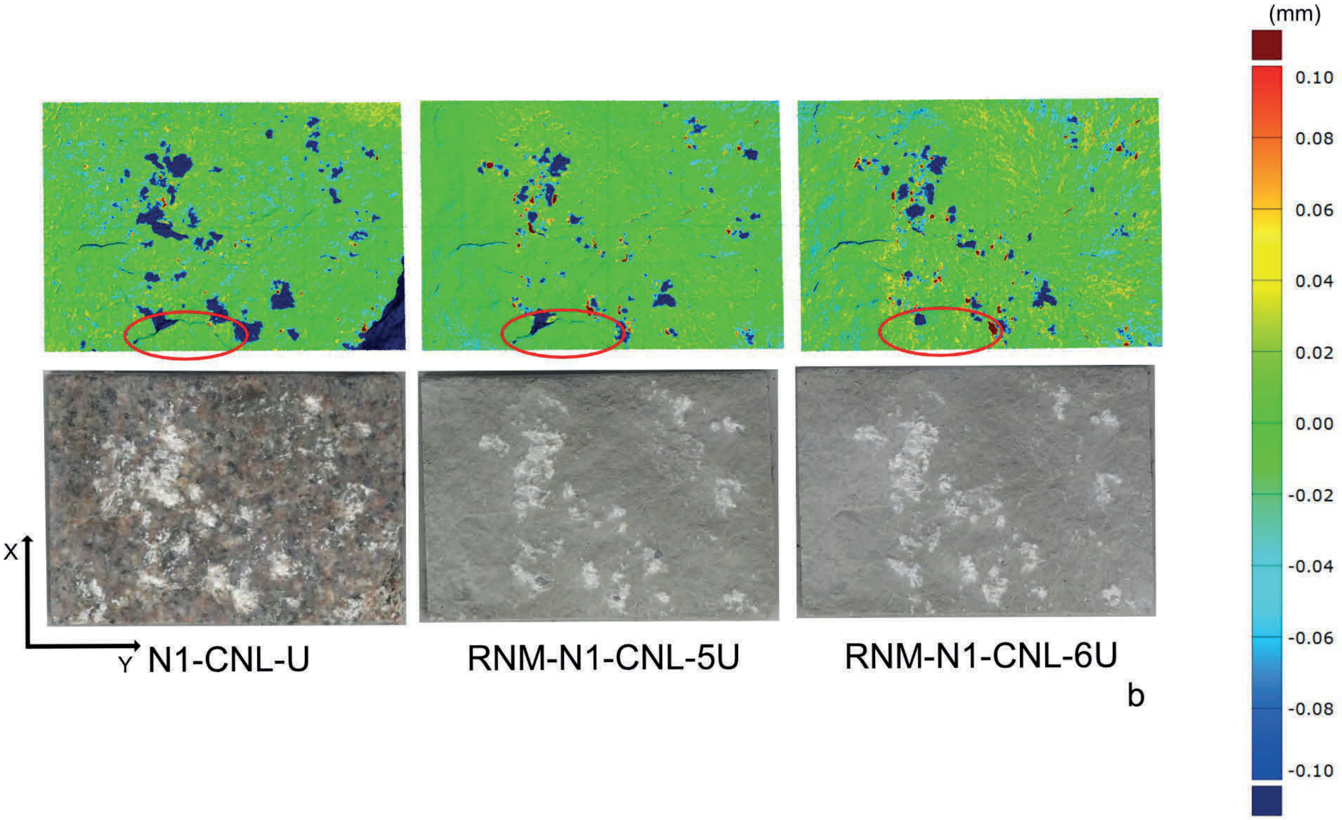

Figure 21 (upper parts): The wear evaluated from surface comparisons of the joint surfaces before and after testing, and photos of (a) the lower parts and (b) the upper parts (Larsson et al. 2023b).

there is no wear in the encircled areas, despite this area of RNM-N1-CNL-6 being in initial contact (Figure 22). This observation further indicates that not all areas in initial contact affect the shear mechanical behaviour. The deviation (encircled in Figure 22) in RNM-N1-CNL-6 can be explained by a fragment that came off the rock joint and got stuck in the silicone during the mould manufacturing process for casting this replica. Before casting, the fragment was peeled off, resulting in the differences in contact pressure distributions shown in Figure 22.

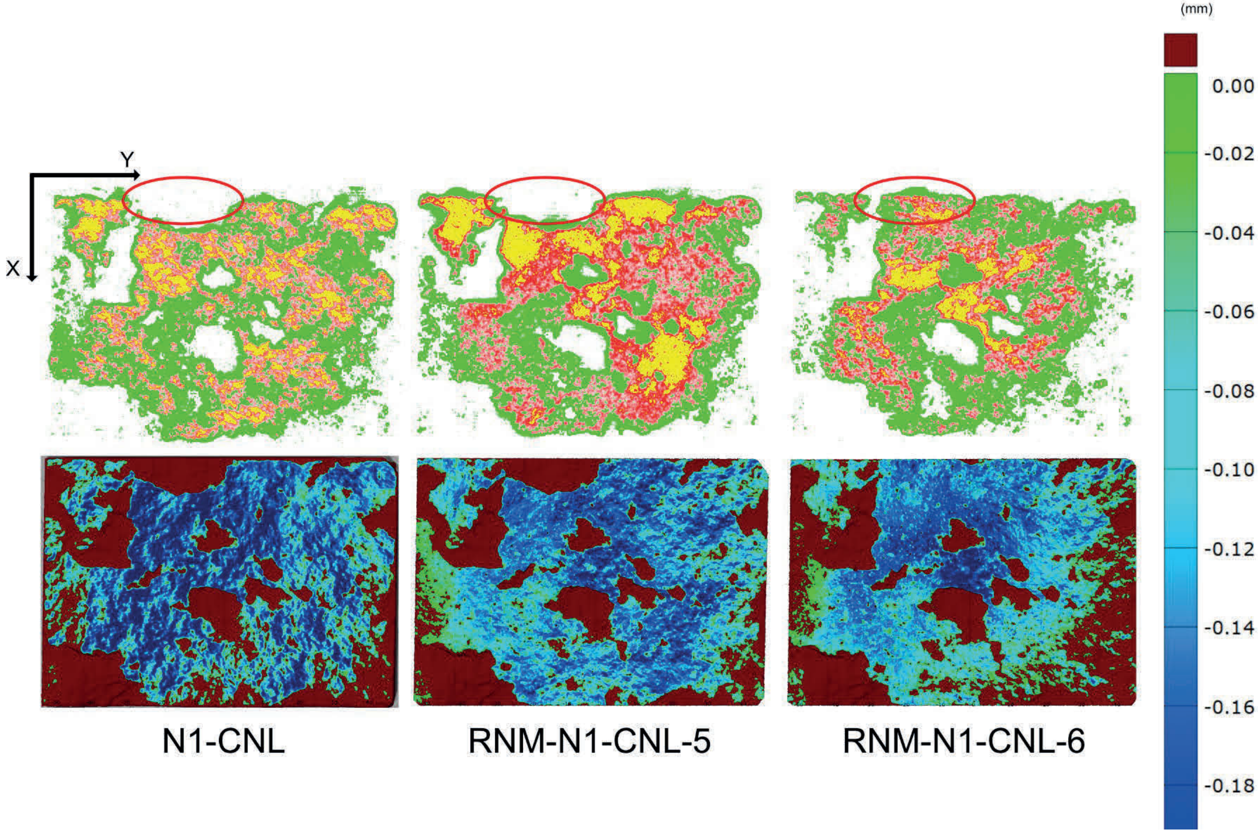

Figure 22: Measured contact pressure distributions with the area from which the fragment came off encircled (upper row), and corresponding contact areas derived from calibration of scanning data with scale (lower row) (Larsson et al.

3.2 Compensation of the influence of the system normal stiffness under the CNS boundary condition

As mentioned in Section 1.4.4, a test system, i.e., all components between the measuring points of the LVDTs, is not infinitely stiff. This means that, in addition to deformations in the joint specimen, undesired, but unavoidable, deformations originating from imperfections in test systems will be measured by the LVDTs. This fact is acknowledged in the "ISRM Suggested Method for Laboratory Determination of the Shear Strength of Rock Joints" (Muralha et al. 2014), which highlights the necessity of having a stiff test system for accurate recording of test data. It is proposed to conduct tests using a high stiffness dummy, i.e., a steel specimen, to enable calibration of test systems. The measured displacements from the dummy test represents deformations in the test system. Under the CNL boundary condition, the influence of deformations in the test system can be corrected after testing by subtracting the displacements at the applied load level recorded during the dummy test from the measured displacements under the CNL direct shear test. This approach has been employed by, e.g., Chryssanthakis et al. (2004) and Dae-Young et al. (2006).

In direct shear testing under the CNS boundary condition, the normal stress applied to the joint should increase proportionally to the dilation, simulating the constraining effect of the rock mass surrounding the joint. The aforementioned imperfections in test systems give rise to undesired but unavoidable stiffnesses. The total effect of these stiffnesses is designated the system normal stiffness, k_{sys}. This stiffness acts simultaneously with the user-defined intended normal stiffness, k_{ns}, set as input to the control system, simulating the effect of the surrounding rock mass. The existence of k_{sys} implies that smaller normal displacements will be measured by the LVDTs than those originating from dilation of the joint, which, in turn, results in a lower normal load being applied compared to what should be the case if the dilatancy resulted only from the joint stiffness and the specimen material.

Since the influence of k_{sys} must be compensated for during CNS direct shear testing, the approach used for the CNL boundary condition is not applicable in this case. Therefore, an approach compensating for the influence of k_{sys} is presented in Larsson et al. (2020). Figure 23a illustrates an ideal, infinitely stiff direct shear test setup with a rock joint specimen subjected to a shear displacement δ_{s} yielding a normal displacement δ_{n} and a dilation angle α. Figure 23b schematically illustrates, from the lower position of the specimen, that too small normal displacements will be measured under the influence of k_{sys}, resulting in a normal load that is too low and needs to be compensated for. Representing the test setup with a model consisting of two springs in series, the following expression is obtained

$$k_{\mathrm{eff}} = \frac{k_{\mathrm{ns}}}{1-\frac{k_{\mathrm{ns}}}{k_{\mathrm{sys}}}}, \tag{20}$$

where k_{eff} is the effective normal stiffness that should be set as input to the control system instead of k_{ns}, to compensate for the influence of k_{sys}. This parameter is derived from the slope of the normal loading versus normal displacement plot from a normal loading test using a steel test dummy. k_{eff} is then calculated from Eq. (20) and set as input to the control system.

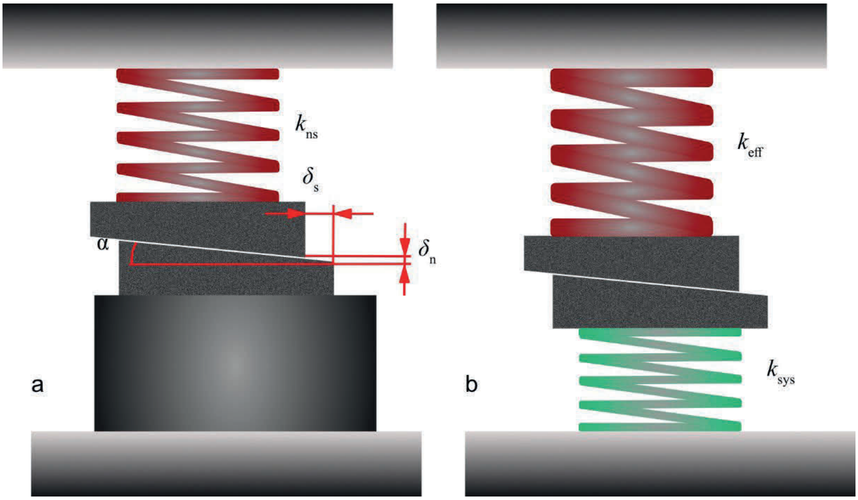

Figure 23: An ideal infinitely stiff direct shear test setup (a) and the effect on the normal displacements under influence of a system normal stiffness (b) (Larsson 2021).

Figure 24 shows the normal stress, σ_n, versus δ_n response from two CNS tests using a steel specimen consisting of two halves forming a planar joint with α equal to 1.8°. In the first test, k_{ns} equal to 15.0 MPa/mm was set as input to the control system. In the second test, the influence of k_{sys} was accounted for by instead setting k_{eff} equal to 22.0 MPa/mm as input to the control system. It is seen, for the specific conditions in this test, that without accounting for k_{sys}, σ_n is about 13% too low at δ_s equal to 8 mm compared to the nominal response. It is also seen that compensating for the influence of k_{sys} by instead setting k_{eff} equal to 22.0 MPa/mm as input to the control system essentially removes the normal stress error.

The application of k_{eff} does not directly correct the normal displacements, but correction can be done by post-processing the test data. Continuing to use the steel specimen consisting of two halves forming a planar joint as an example, the total nominal normal displacement δ_{n_nom} is calculated as

$$\delta_{n\_nom} = \delta_n + \frac{\sigma_n - \sigma_{n0}}{k_{sys}}, \tag{21}$$

where σ_{n0} is the initial normal stress, and the second term on the right-hand side of the equal sign is the effect of k_{sys} on the normal displacements. Figure 25 demonstrates that application of Eq. (21) yields corrected normal displacements. The dotted line represents the inclination of the planar joint in the steel specimen, which as expected coincides with the calculated nominal response. The effective normal stiffness approach was applied in

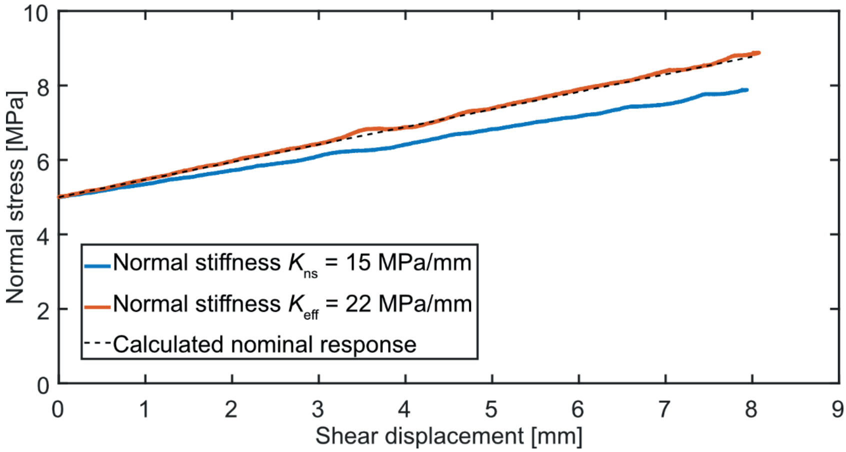

Figure 24: The normal stress versus shear displacement response with and without compensation for the influence of the system normal stiffness (Larsson et al. 2020).

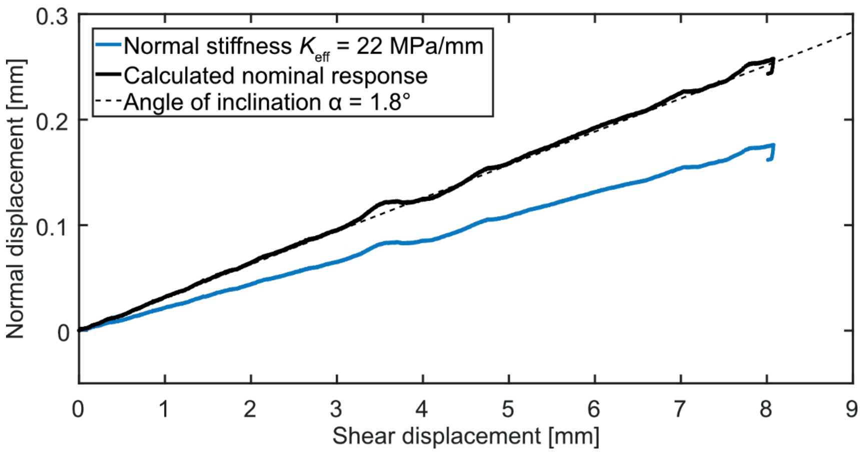

Figure 25: Normal displacement versus shear displacement plots demonstrating the correction of normal displacements, accounting for the system normal stiffness. The dotted line represents the inclination of the planar joint in the steel specimen (Larsson et al. 2020).

all direct shear tests under the CNS boundary condition conducted in the experimental project. In Larsson (2021), the effective normal stiffness approach is validated against the 5 MN shear test equipment, e.g., Jacobsson et al. (2021).

3.3 Determination of shear strength and the effect of specimen size

In the next phase of the study, the experimental program was conducted, applying the approach for compensating for the influence of the system normal stiffness under the CNS boundary condition. Having access to the comprehensive data set, one of the questions of prime interest to investigate was the influence of the specimen size on the shear strength. Despite being a parameter of fundamental importance, a physically based definition of shear strength is missing. In this work, shear strength is defined as the state corresponding to fully mobilized friction. This definition is relevant because it reflects the state of highest shear stress before widespread asperity damage and, hence, irreversible mechanical damage to the joint. Next, an approach identifying the shear stress corresponding to the state of fully mobilized friction is required. As acknowledged by Muralha et al. (1990b), among several others, this state is not always clearly distinguishable.

For this reason, the behaviour of the shear displacement in the time domain is analysed. Three types of shear stress versus time appearances were identified within the test results: a clearly identifiable peak (Figure 26a), a local peak (Figure 26b), and a monotonically increasing behaviour (Figure 26c). Looking at the corresponding shear displacement over time plots in these figures, a pattern common to all appearances is seen. An initial non-linear phase, reflecting the process of gap closure inherent in the test system, i.e., all components, including the specimen, between the measurement points of the LVDTs, is followed by a linear phase. During this phase, elastic deformations are accumulated in the test system. The linear phase is followed by a smooth transition to an additional non-linear phase with an increasing displacement rate, and a simultaneous decreased shear stress rate. This phase indicates initiation of asperity breakage and continues until the state of fully mobilized friction, which coincides with the inflection point in the shear displacement versus time curve, indicated by cross markers in Figure 26a to Figure 26c. At the inflection point, the shear displacement rate reaches its maximum, indicated by the solid black lines in the magnifications in Figure 26a to Figure 26c. After the inflection point the shear displacement rate decreases or becomes essentially constant, indicating a redistribution of the contact points. The point of inflection or tangency coincides with the instant when the second time derivative of δ_s equals zero, i.e., when the change of the displacement rate equals zero. This state is designated $\ddot{\delta}_{s0}$ and corresponds to the state of fully mobilized friction, indicated with cross markers in Figure 26d to Figure 26f.

Using $\ddot{\delta}_{s0}$ to identify the shear strengths in terms of the state of fully mobilized friction, the results for the specimens in the experimental program are presented in Figure 27. Since there are several test results for each parameter combination, it is not clear how to evaluate the influence of specimen size on shear strength. In addition to specimen size,

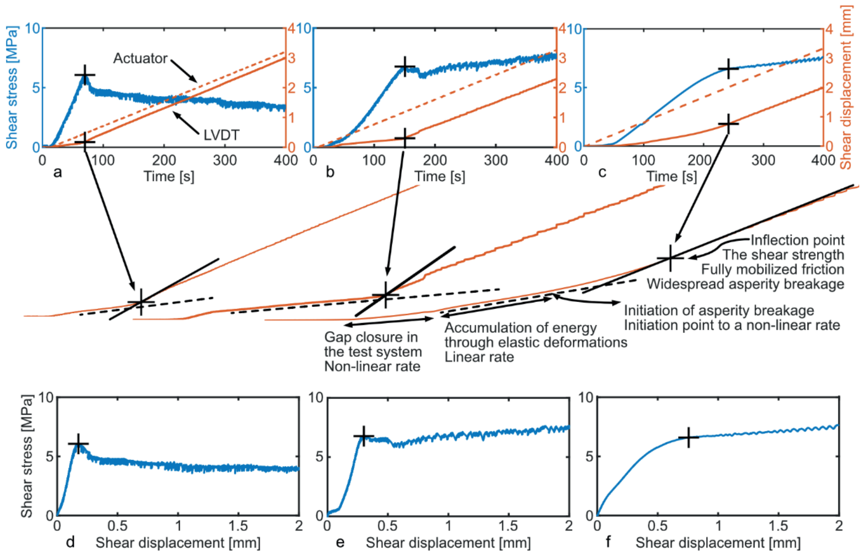

Figure 26: Shear strengths corresponding to the state of fully mobilized friction, derived from the instant when the second time derivative of the shear displacement equals zero. The middle part shows enlarged parts of figure a, b and c.

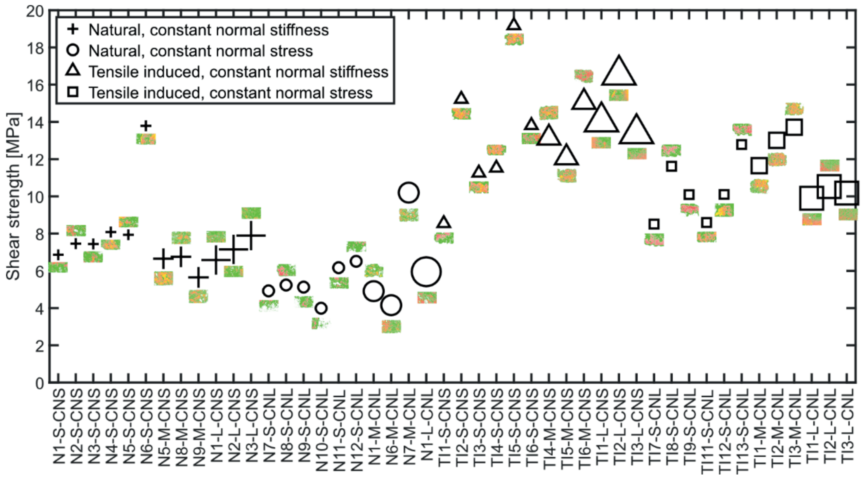

Figure 27: Shear strengths with corresponding digitized images from contact pressure measurements, divided by four groups in which the marker size correlates with the joint size.

the data set consists of two additional factors: joint type (natural and tensile induced) and boundary condition (CNL and CNS). In total, twelve experimental conditions, i.e., unique factor combinations, were tested. Therefore, a method that allows statistical inferences to be made by separating the effect of the factors on the shear strength is required, namely ANOVA. First a model equation is formulated:

$$\tau_{\mathrm{p\_ijkl}} = \mu + \alpha_{\mathrm{i}} + \beta_{\mathrm{j}} + \gamma_{\mathrm{k}} + \varepsilon_{\mathrm{ijkl}}, \tag{22}$$

where $\tau_{\mathrm{p\_ijkl}}$, in terms of response variable, is the shear strength, μ is the mean shear strength of all specimens, α_{i} is the factor representing the joint type, β_{j} is the factor representing the boundary condition, γ_{k} is a factor representing the specimen size, and $\varepsilon_{\mathrm{ijkl}}$ is the error term, with the subscripts $\mathrm{i, j, k, l}$ assuming different values depending on the factor. By formulating the null hypothesis that there are no factor effects (from sample size, joint type or boundary condition) on shear strength, and then applying ANOVA, the results presented in Table 1 were obtained at the 0.05 level of significance. Joint type and boundary condition are very significant, indicated by their high F-values and low P-values, and their null hypotheses are therefore rejected. Consequently, both the joint type and the boundary condition affect the shear strength. On the contrary, specimen size is clearly non-significant, i.e., specimen size does not affect the shear strength.

Table 1: The resulting ANOVA table for the factor effects on the shear strength.

Factor	Sum of squares [MPa²]	Degrees of freedom	Mean square [MPa²]	Reject criterion F >	F	P-value
Joint type	354.965	1	354.965	4.08	77.349	0.000
Boundary condition	64.719	1	64.719	4.08	14.104	0.001
Specimen size	1.211	2	0.606	3.24	0.132	0.877
Error	188.130	41	4.589			

Using the mean shear strength of 9.6 MPa as reference, the effects of joint type and the boundary condition were statistically estimated to: natural, -2.9 MPa; tensile induced, 2.6 MPa; CNL, -1.4 MPa, CNS, 1.0 MPa.

3.4 Determination of shear stiffness and the effect of direct displacement measurements

Following the analyses of shear strength, shear stiffness is investigated in Larsson et al. (2025b). The influence of deformations in the test system is evaluated by comparisons between shear stiffnesses derived from LVDT and optical DIC measurements. LVDTs measure the shear displacements indirectly from the relative position of the shear boxes. DIC measures the displacements directly over the joint. Like shear strength, shear stiffness lacks a consistent and physically based definition, which means that shear stiffness is measured in different manners, see e.g., Grasselli (2001) and Giwelli et al. (2014). In addition, the definition should allow for consistent comparisons between the two measurement techniques.

Figure 28 shows the first 1.5 mm of shearing for three specimens with different characteristics. The shear stress, τ, versus shear displacement, δ_s, plots for both LVDT and DIC measurements are shown in Figures 28a, 28c and 28e. The corresponding δ_s versus time, t, plots are shown in Figure 28b, 28d and 28f. Each row in the figure represents the characteristics of one specimen. From Figure 28a, comparing the LVDT graph with the DIC graph, it becomes clear that the initial non-linear part in the LVDT plot at start of the test originates from imperfections in the test system, which should not be included in the shear mechanical analysis of the joint. Looking at Figure 28c, a non-linear part at start is again observed in the LVDT plot. However, for this specimen, the non-linear part also remains in the DIC plot, although to a lesser extent. The difference in range of the non-linear parts is attributed to imperfections in the test system. The remaining non-linearity in the DIC plot originate from poor joint matching. For this reason, irrespective of measurement technique, the non-linear part should not be included when measuring the shear stiffness. Both graphs in Figure 28e show non-linear characteristics, which, when compared with Figure 28c, are not attributed to poor joint matching.

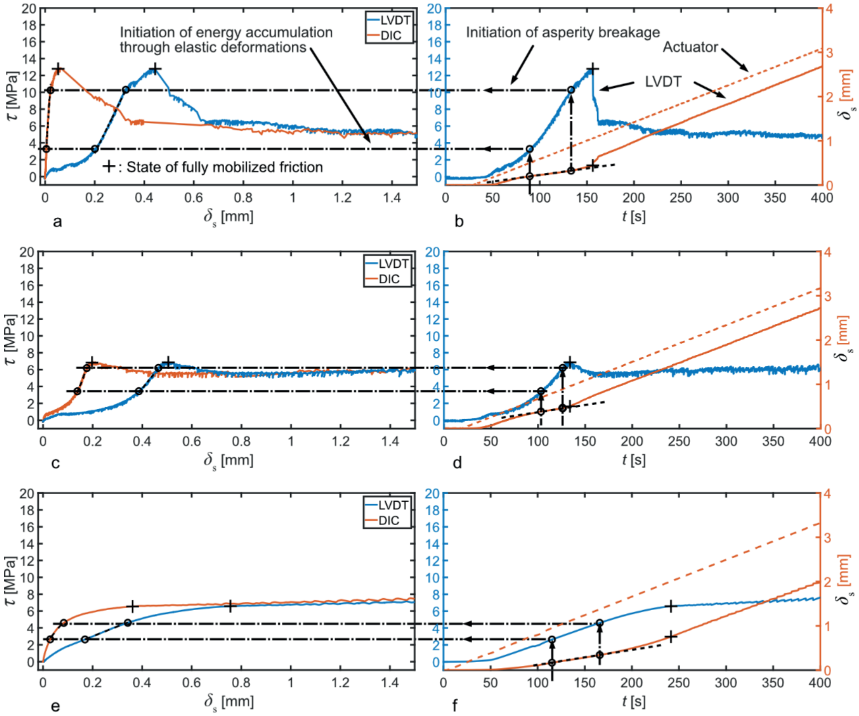

Figure 28: Shear stiffness intervals consistently derived from the time interval in which energy accumulates through elastic deformations.

The question is how to define the shear stiffness and measure it consistently for all three types of appearances. The linear part of the δ_s versus t plots represents a phase of energy accumulation due to elastic deformations. It is observed that the time interval of the linear part in the δ_s versus t plots from LVDT measurements in Figure 28b corresponds to the shear stress interval in the LVDT plot in Figure 28a. This interval is defined by the lower shear stress limit, corresponding to the instant of completion of gap closure of imperfections in the test system, and the upper limit, corresponding to initiation of asperity breakage. The same conclusion can be drawn from comparison of the time interval of linear part in Figure 28d and the corresponding shear stress interval in Figure28c. However, since this joint was initially poorly matched, in this case, the lower stress limit corresponds to the point in time when the joint reached the state of energy accumulation due to elastic deformations after a gradual increase in degree of interlocking.

The slope of the linear part of the δ_s versus t plots describes the characteristics of the test system, to which the joint is part of. Inferences from the slope about the shear stiffness can therefore not be made directly, but indirectly by linking to the interval of the linear part of the slope to the corresponding shear stress interval. Consequently, the shear stiffness should be determined from the shear stresses in the time interval during which shear displacement rate is constant, designated $\dot{\delta}_{s\_const}$. The true shear stiffnesses will be measured as they are derived from the intervals containing only elastic deformations, making this approach physically based. In addition, the approach allows for consistent evaluation of both LVDT and DIC displacement measurements and is applicable regardless of the appearance of the τ versus δ_s curve. Figures 28e and 28f show that the approach is also applicable to joints with a non-linear τ versus δ_s behaviour.

The shear stiffness is measured as the shear stress range divided by the corresponding shear displacement range, defined by the limits of the evaluation interval. It is observed in Figures 28a, 28c and 28e that the shear stiffnesses measured from LVDT measurements are lower than measured from DIC measurements. The reason is that LVDT measurements, in addition to deformations in the joint, also contain deformations in the test system outside the joint. Consequently, the shear stiffness will be underestimated when measured from LVDT displacements. In this study, the shear stiffness is underestimated from LVDT measurements, on average by a factor of five relative to DIC measurements yielding a mean equal to 217 MPa/mm. The variation is large, with a maximum ratio of fifteen.

Figure 29 shows the results of the shear stiffnesses derived from DIC measurements along with digitized images from contact pressure measurements. The results from analysis of variance presented in Table 2 shows that there is an effect of joint type (natural or tensile induced) and joint size on the shear stiffness, whereas not from boundary condition (CNL or CNS).

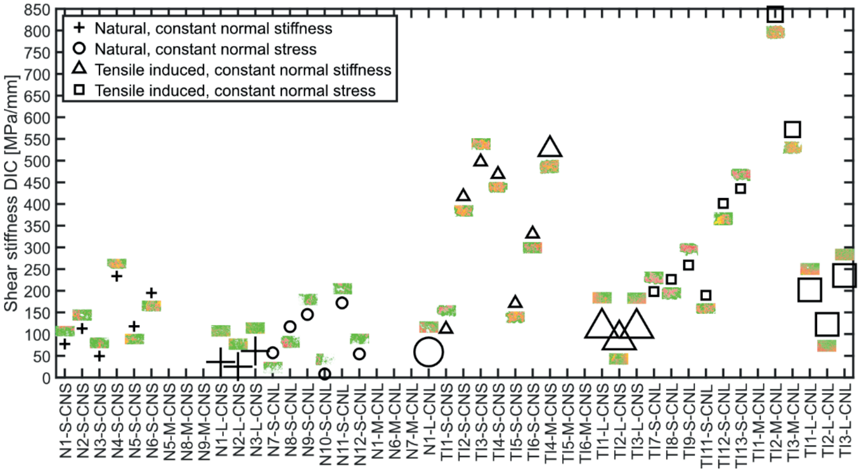

Figure 29: Shear strengths with corresponding digitized images from contact pressure measurements, divided by four groups in which the marker size correlates with the joint size.

Table 2: The resulting ANOVA table for the factor effects on the shear stiffness.

Factor	Sum of squares [(MPa/mm)^2]	Degrees of freedom	Mean square [(MPa/mm)^2]	Reject criterion F >	F	P-value
Joint type	239979.260	1	239979.260	4.17	27.750	0.000
Boundary condition	6557.725	1	6557.725	4.17	0.758	0.391
Joint size	113021.089	1	113021.089	4.17	13.069	0.001
Error	259437.301	30	8647.910			

4. DISCUSSION

In this section, the results are discussed with respect to the research questions presented in Section 1.5. The research questions are discussed separately in Section 4.1 to Section 4.5. A concluding discussion is presented in Section 4.6

4.1 Uncertainties in direct shear testing of rock joint replicas (RQ 1)

The application of direct shear testing of rock joint replicas is extensive, as exemplified by the investigation of the influence of anisotropy and loading on shear strength by Um (1997), the influence of the joint roughness on the shear behaviour by Jiang et al. (2019), and the development of a peak shear strength criterion based on three-dimensional surface description by Liu et al. (2018). However, the mechanical replicability, i.e., the impact of geometrical variation of replicas on shear mechanical behaviour and the difference in shear mechanical behaviour between replicas and rock joint when using replicas in experimental studies receives generally very little attention in the literature. This should be noticed. Uncertainties will remain hidden unless the experimental practice of conducting several tests for each parameter combination and reporting individual results is followed. The additional testing cost is small compared to the costs of drawing false conclusions by leaving the accuracy and the precision of the results unknown.

Efforts should be made to develop replica materials that mimic the mechanical characteristics of the joint. For successful application of replicas, the elastic and the fracture mechanical properties in terms of deformational behaviour, but not necessarily with respect to fracture energy, between replica and rock material must be equal. When plotting stresses and displacements, this means that replicas will mimic the shear mechanical behaviour, although not necessarily with respect to stress levels. Under such conditions, models can be developed and validated (checked to ensure they correctly describe the parameter or process they were developed for) against replica results in parametric studies. This is possible provided that geometrical quality assurance parameters, as suggested in Larsson et al. (2023a), combined with a geometrical quality assurance method, as suggested in Larsson et al. (2023b), are applied. Model verification can subsequently be made against data from rock joint tests, i.e., to check that the models also accurately describe the parameter or process of rock joints.

The versatile use of replicas has been exemplified and summarized as follows. In Section 1.4.6, the possibilities of investigating the influence of waviness superposed onto roughness on the shear mechanical behaviour was highlighted. In Section 3.1, the possibility of investigating why some areas despite being in initial contact, are not active during shearing was shown. This is also discussed in Larsson et al. (2023b). Another example refers to Figure 21. All joints have essentially identical morphology and wear areas, but a higher degree of wear is observed, and a higher peak shear stress is noted for the rock specimen at equal shear displacement of the rock joint and the replicas. This indicates that more energy was required before rupturing the rock joint, suggesting higher toughness of the granite material. In Larsson et al. (2023b), an analysis using the shear strength criterion in Eq. (2) yielded that the difference in wear between rock and replicas could not be attributed to differences in compressive strength or basic friction angle. A possible explanation could be that toughness is a parameter that needs to be included in shear strength criteria. With reference to the results presented in Larsson et al. (2023a) and Larsson et al. (2023b), and the examples provided here, it is worth investing resources in developing replica materials, combined with geometrical quality assurance of rock joint replicas. This approach will ensure mechanical replicability, allowing us to isolate and study a wide range of research questions separately under controlled conditions.

4.2 Uncertainties in control during direct shear testing (RQ 2)

Different types of uncertainties related to control during direct shear testing exist. One type of uncertainty occurs when the size of the joint surface is unintentionally changed. This results in the actual joint area being smaller than that calculated from the nominal set as input to the control system, leading to errors in the measurements of the stresses. In Section. 1.4.4, breaking of trailing edges, as also noted by e.g., Ohnishi et al. (1993) and Bahaaddini (2017), is highlighted. In the experimental project related to this study, before casting, steel supports were glued to the trailing edges closely to the traces of the joints, to minimize the risk of breakage during shearing, which is shown in Larsson et al. (2025a). Before this action was implemented, typically breakage occurred at shear displacements shortly after the shear strength was reached.

A second type of uncertainty, noted during CNS direct shear testing, is resonance. During shearing, as the normal stiffness of the joint changes due to dilation, a point could be reached when the normal stiffness of the joint coincides with the normal stiffness of the normal loading system, causing resonance. Resonance is avoided by tuning the PID (Proportional – Integral – Derivative) controller. Under the CNS boundary condition, testing specimens with normal stiffnesses not previously tested, such as new specimen material or size, it is difficult to tune the PID parameters in advance due to the normal stiffnesses occurring during shearing being unknown. The consequence is a sudden normal load drop under oscillation of the normal load. The problem was solved by tuning the proportional (P) component until the oscillations disappeared, as noted in Larsson et al. (2025a). Oscillating normal load could affect the result and should be paid attention to in the result evaluation.

The influence of the normal stiffness of the test system is a source of error, which causes too low normal loads being applied during testing under the CNS boundary condition. The need of accounting for the influence of the normal stiffness of the test system increases with decreasing system normal stiffness, k_{sys}, which follows from an increased value of k_{eff} according to Eq. (20). Consequently, the error varies between test setups and is dependent on the user-defined intended normal stiffness, k_{ns}, set as input to the control system. An error of 13% was measured at about 8 MPa normal stress with k_{ns} equal to 15 MPa/mm for the 300 kN GCTS direct shear testing equipment, as shown in Section

3.2, and discussed in Larsson et al. (2020). The normal load error for the RISE direct shear testing equipment with a 5 MN normal load and shear capacity was measured to be 11% at about 28 MPa normal stress with k_{ns} equal to 10 MPa/mm as reported in Larsson (2021). The normal load errors basically were eliminated by application of the suggested approach presented in Larsson et al. (2020). Figure 24 shows that the normal load error increases with shear displacement, which is attributed to the increased normal load originating from dilatancy. It is therefore particularly important to compensate for the normal load error in the ultimate shear stress state. No similar investigations have been found in the literature, but the fact that these errors arise under system normal displacements in the order of a few tenths of millimetres, indicates the importance of accounting for the influence of k_{sys} conducting laboratory direct shear testing under the CNS boundary condition.

4.3 Uncertainties in determination of parameters (RQ 3)

The suggested definitions of shear strength (the state corresponding to fully mobilized friction) and shear stiffness (derived from intervals containing only elastic deformations) can be generalized to apply to any material and test condition where the specimen undergoes plastic deformations. Combining these definitions with the suggested approaches for determining shear strength (from when the change of displacement rate equals zero, designated $\ddot{\delta}_{\mathrm{s0}}$) and shear stiffness (determined from the time interval during which shear displacement rate is constant, designated $\dot{\delta}_{\mathrm{s\_const}}$) uncertainties in determination of these parameters can be reduced.

The relevance of establishing these physically based definitions and approaches is demonstrated by the results of the experimental program. All three types of appearances of the relation between shear stress and shear displacement reported by Muralha et al. (1990b) can be seen in the results presented in Larsson et al. (2025a): graphs with a clearly identifiable peak shear stress, with a local maximal shear stress and with a monotonically increasing trend. Determining the shear strength from $\ddot{\delta}_{\mathrm{s0}}$ means that the shear strength can be consistently determined, regardless of appearance. From the experimental results presented in Larsson et al. (2025a), this turns out to be of particular relevance to the natural specimens sized 300 mm × 500 mm tested under the CNS boundary condition, all of which exhibit a monotonically increasing trend. These results are unique since this is the first time large rock joints have been tested at 5 MPa initial normal stress under the CNS boundary condition, representing states occurring at depths of several hundreds of meters, relevant to, for example, deep mining and nuclear waste repositories. Presuming that these results are representative of full-scale rock joints, this demonstrates the importance of having an approach for the consistent determination of the shear strength of joints exhibiting a monotonically increasing trend.

Regarding the measurement of shear stiffness, the issue of non-linear elastic behaviour is noted by Day et al. (2017). This behaviour is also observed in the results of the natural specimens sized 300 mm × 500 mm, regardless of boundary condition. The applicability of the approach determining the shear stiffness from $\dot{\delta}_{\mathrm{s\_const}}$ to a non-linear elastic behaviour is demonstrated in Larsson et al. (2025b). In analogy with the statement about shear strength, with reference to the uniqueness of the experimental results and presuming that these results are representative of full-scale rock joints, the importance of having an approach for the consistent determination of the shear stiffness of joints exhibiting a non-linear elastic behaviour is demonstrated in Larsson et al. (2025b).

Both approaches for the determination of shear strength and shear stiffness, respectively, have been derived from direct shear test results on granite, a high-strength crystalline rock material, under a high constant or initial normal stress of 5 MPa. Determination of the shear strength from $\ddot{\delta}_{\mathrm{s0}}$ requires identification of the point of inflection or tangency in a shear displacement versus time plot. Measurement of the shear stiffness from $\dot{\delta}_{\mathrm{s\_const}}$ requires identification of the interval during which the relation between shear displacement and time is linear. The question is whether these two types of characteristics are distinguishable under lower normal stresses, weaker materials, or a combination of lower stress and weaker material.

Starting with the point of inflection or tangency from which the shear strength is determined. Since this point reflects the state of widespread asperity damage, plasticity of the joint is a prerequisite for application of the approach, which should be the case of most practical applications. Even under low normal loads, it should be possible to identify a transition point from a higher shear displacement rate to a lower or constant displacement rate, although originating from a limited extent of asperity damage. The same applies to low-strength materials requiring low loads to progress shearing. In this case, the shear displacement over time signal will more directly represent the behaviour of the joint. The low shear load implies that there will be no or limited contributions to measured shear displacements from the test system outside the joint. In summary, as long as there is a non-linearity in shear stress versus shear displacements graphs, the approach should be applicable, even for low normal stresses and low-strength materials. Under such circumstances the appearance of the shear displacement over time graph is expected to show continuous non-linear behaviour, as in Figure 26c.

The interval during which the relation between shear displacement and time is linear, required to measuring the shear stiffness, should be distinguishable even under low normal loads or using low-strength materials. Under such circumstances, since the shear load required to progress shearing is too low to generate elastic deformations outside the joint, the slope of the linear part corresponding to the evaluation interval, is expected to be like the slope of the actuator (c.f. Figure 28b). This means that the shear displacement over time graph will be linear from the start. In such cases the lower point of the evaluation interval coincides with the origin. Even though the shear displacement over time graph would have the same slope as the actuator from the start, the upper point of the evaluation interval should be distinguishable from the point where non-linear behaviour starts, followed by a small notch in the graph, before the slope returns to its original state. Thus, it should be possible to generalize the suggested approaches to any material and test condition where the specimen undergoes plastic deformations.

4.4 Uncertainties in data collection (RQ 4)

A major contributor to uncertainties in data collection is the measurement of displacements. The uncertainty arises from the fact that no test system is infinitely rigid. Therefore, in addition to deformations in the joint, deformations in the materials and contact surfaces in the test system outside the joint will be captured in conventional indirect displacement measurements. This uncertainty is well-known, as acknowledged by Jacobsson et al. (2012) among several others. Therefore, unique setups were developed allowing measurement of displacements directly over the joint in both direct shear test setups using optical DIC measurements. The setups and the results from comparisons between conventional indirect and direct DIC displacement measurements are presented in Larsson et al. (2025b).

The results show that the direct shear stiffness derived from conventional indirect measurements is on average by a factor of five lower than measured directly over the joint. The results are unique in terms of application of DIC for the measurement of shear stiffness, which means that the DIC direct measurements cannot be discussed in relation to other studies. In a few studies, the displacements were measured directly over the joint using other techniques. One of these studies are presented in Bandis (1980) where the results from standard dial arrangement were compared with the results from dial arrangement directly over the joint on sandstone. The direct measurements were reported to be two to three times smaller.

To obtain complementary information on the reasonableness of the DIC direct displacement measurements, the normal stiffness of intact rock derived from a uniaxial compression test was compared with the normal stiffness of a rock joint derived from a normal loading test using DIC. The modulus of elasticity of intact rock from normal loading was measured to be 73 000 MPa. Using an evaluation length of 3 mm, corresponding to the virtual extensometer length used in evaluation of the DIC measurements, a normal stiffness of $73\ 000/3$ equal to 24 333 MPa/mm is obtained. This value is between seven and fifteen times higher than the rock joint normal stiffness obtained from DIC measurements, ranging between 1640 MPa/mm and 3480 MPa/mm. This indicates that the small displacements measured with DIC are reasonable. The presented shear stiffnesses derived from direct displacement measurements, call for a review of the parameters in theoretical models for predicting shear stiffness, and potentially even of the models themselves.

Having acquired the equipment required for DIC direct displacement measurement, the setup time should not be an issue when distributing the cost over several specimens. The post-processing of digital images requires additional time when done manually compared to the evaluation of conventional data from displacement gauges. However, the post-processing could be automated by scripting, making DIC direct displacement measurements a complement to conventional indirect measurements in laboratory testing. A difference in displacement on the order of hundreds of millimetres will affect the measured stiffness. For this reason, measuring the shear stiffness using a least squares fit is deemed better than using the secant method.

4.5 Uncertainties in analysing size effects (RQ 5)

A prerequisite for reducing uncertainties in studies investigating the influence of joint size on shear strength and shear stiffness is access to reliable data. The data from the extensive experimental project (the POST project described in Section 1.1), which was conducted in parallel with this study and used to evaluate the size effect, is free from the sources of uncertainties that affected previous studies. This reliability was achieved by performing several tests for each parameter combination, ensuring that each specimen was tested only once, using the same material, under controlled laboratory conditions, and across a range of specimen sizes not previously examined under these conditions.

A second uncertainty lies in the evaluation of the data. In addition to having access to a data set that allows for statistical evaluation, a proper statistical method must be employed. The data used in this study consists of twelve unique combinations of specimen size, joint type and boundary condition, making it difficult to make statistical inferences just by calculating means and standard deviations. Therefore, ANOVA was applied, which allows for statistical comparisons between more than two groups. ANOVA is an established statistical method which, when applied to the data set, not only allowed for making statistical inferences from joint size, but also from joint type and boundary condition. The results from the ANOVA presented in Larsson et al. (2025a) clearly support that joint type and boundary condition influence shear strength, whereas joint size does not. The results from ANOVA presented in Larsson et al. (2025b) support that joint size and joint type influence shear stiffness, whereas boundary condition does not.

The results of an introductory investigation in Larsson et al. (2025a) indicate that the distribution of inclinations of asperities in initial contact relates to shear strength but does not fully explain the coupling between morphology and shear strength. For same joint type and boundary condition, no correlation between initial contact pressure distribution and shear strength could be observed, whereas the results presented in Larsson et al. (2025b) show a correlation between initial contact pressure distribution and shear stiffness. Dilation effects explain why there is an influence of boundary condition on shear strength, but not on shear stiffness. In Larsson et al. (2025b) it is shown that dilation starts at initiation of asperity breakage, which is outside the evaluation interval of shear stiffness. Asperity breakage occurring between the state corresponding to the upper evaluation point of shear stiffness and the state of fully mobilized friction, changes the contact conditions. This could explain why the initial contact pressure distribution correlates well with shear stiffness, whereas not with shear strength.

It has been shown in the analysis of the results from the performed experimental program that the specimen size does not influence the shear strength. For the granite material and the boundary conditions used in the experimental program, this means that any specimen size can be used in laboratory direct shear testing when developing theoretical models predicting shear strength. However, since the variability increases with decreasing specimen size, a larger number of specimens is required as the specimen size decreases to obtain the same confidence as for larger specimens. Nevertheless, it is recommended that theoretical models are validated against different sample joint sizes to gain confidence in predictions of the shear strength of full-scale rock joints.

Since shear stiffness is size dependent, theoretical models require validation against different sample sizes to gain confidence in predictions of full-scale rock joints. As with shear strength, since the variability increases with decreasing specimen size, a larger number of specimens is required as the specimen size decreases to obtain the same confidence as for larger specimens.

4.6 Discussion summary

The data from the experimental project consists of laboratory direct shear testing results combined with contact pressure measurements taken before testing, and 3D scans of the joint surfaces before and after testing, that is more extensive and complete than previously presented data in the literature. Together with the suggested and applied approaches presented in this work, excellent prerequisites exist for deriving novel and deeper insights into the factors influencing the shear mechanical behaviour of rock joints, and how they operate.

Of primary interest is to investigate the accuracy and precision of some commonly used shear strength criteria when applied to the data set. More specifically, the applicability of CNL shear strength criteria to high normal stresses (5 MPa), representative of deep underground excavations, should be evaluated. The applicability of these criteria to data from CNS direct shear testing should also be investigated, potentially confirming the need for specific criteria for this boundary condition.

Joint matching described in terms of initial aperture is a parameter that is incorporated in some shear strength criteria. The aperture distribution varies with normal stress and is not straightforward to measure. A suggested first task is therefore to derive a method for calibrating scanning data against contact pressure measurements, followed by a sensitivity analysis of predicted shear strengths from variations in aperture input parameters.

Some factors highlighted in this study need further attention. Scanning data before direct shear testing calibrated with contact pressure measurements, can be used for detailed analysis of initial contact conditions. This, combined with analysis of calibrated scanning data after direct shear testing and photo documentation, can be used to determine areas in initial contact, the geometries of these areas, and why some of them are not active during shearing. Such analyses are required for understanding of the shear mechanical behaviour after fully mobilized friction, but are also important for understanding the process from initiation of asperity breakage to fully mobilized friction, which is necessary for understanding the geometrical factors governing the state of fully mobilized friction.

Geometrically quality assured replicas manufactured from the same rock joint, but made of different materials, can be used to investigate whether a parameter describing toughness possibly should be added to shear strength criteria or replace tensile or compressive strength.

Fully matched replicas manufactured from the same mould, and thereby having identical roughness but different waviness, obtained by imposing deformations to the mould before casting, which requires deformable moulds such as silicone, can be used to study the effect from waviness superposed onto roughness.

The suggested approaches for determining shear strength and shear stiffness have been derived from direct shear testing of granite under 5 MPa initial normal stress. The applicability of these parameters should therefore be evaluated against other rock materials and initial normal stresses.

The optical DIC displacement measurements directly over the joint have demonstrated substantial underestimation of the shear stiffness when derived from conventional indirect LVDT displacement measurements. The normal stiffness controls parameters such as settlement and hydraulic conductivity, which are also derived from displacement measurements. Therefore, the influence of the normal stiffness of the test system should be investigated using direct DIC displacement measurements.

The results from the areas investigated, as defined by the research questions, all contribute to improved accuracy in various phases of the model development process. In the long-term perspective, improved accuracy of theoretical models contributes to a sustainable society by allowing for better predictions of the load bearing capacity, positively impacting various parts of the construction process.

A concluding reflection: Theoretical models should predict shear mechanical behaviour with the highest possible accuracy applicable under engineering conditions. However, in the development phase, they should accurately predict the shear mechanical behaviour of individual specimens. Using complete and comprehensive data sets from laboratory testing, physically based parameters should gradually be added until the behaviour of individual specimens is predicted and the physics behind the behaviour is fully understood. From this state, controlled model simplifications can be made to make the models applicable to engineering applications.

5. CONCLUSIONS

Several approaches have been presented to reduce or eliminate uncertainties in the data from direct shear testing of rock joints, which, in turn, facilitates the development of improved models describing the shear mechanical behaviour of rock joints.

Uncertainties associated with the specimen preparation process of rock joint replicas can be reduced through geometrical quality assurance. Two quality assurance parameters have been presented: one, σ_{mf}, capturing morphological deviations and the other, $\boldsymbol{V}_{\mathrm{Hp100}}$, deviations in orientation. The application of these quality assurance parameters has demonstrated that it is possible to manufacture replicas with essentially identical geometries and shear mechanical behaviour, targeting RQ 1. Using proper replica material, the application of the suggested quality assurance parameters facilitates the reliable use of replicas in parametric studies.

Two approaches related to control and data collection in laboratory direct shear testing have been presented. The first approach addresses RQ 2. Application of the effective normal stiffness approach basically eliminates the normal load error, which originates from unavoidable deficiencies in test systems, during direct shear testing under the CNS boundary condition.

The second approach addresses RQ 4. Setups for direct DIC displacement measurements directly over traces of joints have been developed. Comparisons between data collected from conventional indirect LVDT displacement measurements, and optical DIC direct displacement measurements, have clearly shown that direct displacement measurements are required for accurate determination of shear stiffness. The shear stiffnesses derived from indirect displacement measurements are on average by a factor of five lower than derived from direct displacement measurements.

Two areas reducing uncertainties in result analysis have been investigated. Firstly, physically based definitions and approaches for the consistent determination of shear strength, $\ddot{\delta}_{\mathrm{s0}}$, and shear stiffness, $\dot{\delta}_{\mathrm{s\_const}}$, have been presented, targeting RQ 3. Secondly, addressing RQ 5, the statistical approach of analysis of variance has been used to make statistical inferences from joint type, boundary condition and specimen size on shear strength and shear stiffness, respectively. According to the data analysed in this work, joint size does not affect shear strength, whereas boundary condition does not affect shear stiffness.

Since no model is more accurate than the data it is validated against, reduced uncertainties associated with direct shear testing is a prerequisite for the development of accurate theoretical models, and an increased understanding of the shear mechanical behaviour of rock joints. In a wider perspective, improved theoretical models imply better predictions of the load bearing capacity of rock mass. This means better control of safety margins, which improves working environments during construction and operation. An improved control of load bearing capacity also contributes to increased construction efficiency, reduced negative environmental impact, safer urban transportation systems and more robust infrastructure.

6. ACKNOWLEDGEMENTS

I would like to acknowledge the financial contribution from the Rock Engineering Research Foundation, BeFo (grant proposals BeFo 391 and BeFo 430), which provided me with the opportunity to carry out the research presented.

SKB (Swedish Nuclear Fuel and Waste Management Co, Sweden) and NWMO (Nuclear Waste Management Organization, Canada) are acknowledged for their financial support of the experimental program, within which the experimental data that forms the basis for this research work was generated.

I thank the Rock Engineering Research Foundation reference group for their engagement which added perspectives and valuable input to this work: Christer Andersson (Ramboll), Axel Bolin (The Swedish Transport Administration), Mattias Roslin (The Swedish Transport Administration), Per Tengborg (The Rock Engineering Research Foundation), Patrik Vidstrand (The Rock Engineering Research Foundation) and Thomas Wettainen (LKAB).

I also thank Denis Jelagin for reviewing the doctoral thesis and adding valuable comments.

Ignacio Pérez-Rey is acknowledged not only for his contributions as a co-author, but also the friendship we developed in parallel with our cooperation in the research work.

I appreciate the good cooperation with the staff at Söder's Stonemasonry and their ability to find setups that maintained the joints undisturbed during cutting, which was an important part of the experimental work.

Finally, I express my gratitude to all colleagues at RISE who have contributed to different parts of the experimental work: Caroline Hanquist, Jesper Olsson and Natalie Williams Portal for their work in the specimen preparation process; Magnus Herbertsson and Jörgen Spetz for the accomplishment of the scans, Tom Lindström and Pooya Tabib for assisting in the tests in the 5 MN setup; and Carl-Magnus Jakobsson and Reine Weijmer for the rigging work in the 5 MN test setup.

7. REFERENCES

Abolfazli M. Fahimifar A, 2020 “The effects of rock joint characteristics and normal stress level on the stiffness of rock joints”. Arabian Journal of Geosciences, no. 13, 984. https://doi.org/10.1007/s12517-020-05934-2

Bahaaddini, M, 2017 “Effect of boundary condition on the shear behaviour of rock joints in the direct shear test”. Rock Mechanics and Rock Engineering, no. 50, pp. 1141–1155. https://doi.org/10.1007/s00603-016-1157-z

Barton N, 1973 “Review of a new shear-strength criterion for rock joints”. Engineering Geology, no. 7, pp. 287–332. https://doi.org/10.1016/0013-7952(73)90013-6

Barton N, Choubey V, 1977 “The shear strength of rock joints in theory and practice”. Rock Mechanics, no. 10, pp. 1–54. https://doi.org/10.1007/BF01261801

Bandis S, 1980 “Experimental studies of scale effects on shear strength, and deformation of rock joints”. Dissertation at the University of Leeds.

Bandis S, Lumsden AC, Barton NR, 1981 “Experimental studies of scale effects on the shear behaviour of rock joints”. International Journal of Rock Mechanics and Mining Sciences & Geomechanics Abstracts, no. 18, pp. 1-21. https://doi.org/10.1016/0148-9062(81)90262-X

Casagrande D, Buzzi O, Giacomini A, Lambert C, Fenton G 2018 “A New stochastic approach to predict peak and residual shear strength of natural rock discontinuities”. Rock Mechanics and Rock Engineering, no. 51, pp. 69-99. https://doi.org/10.1007/s00603-017-1302-3

Chryssanthakis P, 2004 “Oskarshamn site investigation, Drill hole: KSH01A The normal stress and shear tests on joints”, SKB Report No. P-04-185 SKB Stockholm, pp. 15-16.

Dae-Young K, Byung-Sik C, Jin-Suk Y, 2006 “Development of a direct shear apparatus with rock joints and its verification tests”. Geotechnical Testing Journal 29, no. 5, Paper ID GTJ12553, www.astm.org

Day JJ, Diederichs MS, Hutchinson DJ, 2017 “New direct shear testing protocols and analyses for fractures and healed intrablock rockmass discontinuities”. Engineering Geology, no. 229, pp. 53–72. https://doi.org/10.1016/j.enggeo.2017.08.027

Giwelli, AA, Sakaguchi K, Gumati A, Matsuki K. 2014 “Shear behaviour of fractured rock as a function of size and shear displacement”. Geomechanics and Geoengineering, no. 9, pp. 253-264. https://doi.org/10.1080/17486025.2014.884728

GOM Inspect, 2018, Rev. 111035, Build 2018-07-11, Zeiss https://www.zeiss.com/metrology/en/software/zeiss-inspect.html

Grasselli G, 2001 “Shear strength of rock joints based on quantified surface description”. Dissertation at Ecole Polytechnique Federale De Lausanne

Grasselli G, Wirth J, Egger P, 2002 “Quantitative three-dimensional description of a rough surface and parameter evolution with shearing”. International Journal of Rock Mechanics and Mining Sciences, no. 39, pp. 789-800. https://doi.org/10.1016/S1365-1609(02)00070-9

Grasselli G, Egger P, 2003 “Constitutive law for the shear strength of rock joints based on three-dimensional surface parameters”. International Journal of Rock Mechanics and Mining Sciences, no. 40, pp 25-40. https://doi.org/10.1016/S1365-1609(02)00101-6

Haberfield CM, Szymakowski J, 2003 “Application of large scale direct shear testing. Australian Geomechanics”. News journal of the Australian Geomechanics Society no: 38(1), pp: 29–39. https://search.informit.org/doi/10.3316/informit.814329096425742

Hencher SR, Toy JP, Lumsden AC, 1993 “Scale dependent shear strength of rock joints”. Paper presented at the second International Workshop on Scale Effects in Rock Masses. Pinto da Cunha (ed.). Balkema, Rotterdam. ISBN 90 5410 322 1

Hossaini AK, Babanouri N, Nasab SK, 2014 “The influence of asperity deformability on the mechanical behavior of rock joints”. International Journal of Rock Mechanics and Mining Sciences no. 70, pp. 154-161 https://doi.org/10.1016/j.ijrmms.2014.04.009

Huang M, Hong C, Du S, Luo Z, 2020 “Experimental technology for the shear strength of the series-scale rock joint model”. Rock Mechanics and Rock Engineering, no. 53, pp. 5677–5695. https://doi.org/10.1007/s00603-020-02241-w

Högdahl K, Andersson, UB, Eklund O (eds.), 2004 “The Transscandinavian Igneous Belt (TIB) in Sweden: A review of its character and evolution”. Geological Survey of Finland, Special Paper 37.

Indraratna B, Oliveira DAF, Brown ET, 2010 “A shear-displacement criterion for soil-infilled rock discontinuities”. Géotechnique no. 60(8), pp. 623-633 https://doi.org/10.1680/geot.8.P.094

Jacobsson L, Glamheden R, Hakami E, Olofsson I, 2012 “Rock mechanics laboratory testing in SKB site investigation program”. In ISRM EUROCK (pp. ISRM-EUROCK). ISRM. 2012, May

Jacobsson L, Mas Ivars D, Kasani HA, Johansson F, Lam T, 2021 “Experimental program on mechanical properties of large rock fractures”. IOP Conference Services: Earth and Environmental Science. 833 012015. https://doi.org/10.1088/1755-1315/833/1/012015

Jiang Y, Wang Y, Yan P, Luan H, Chen Y, 2019 “Experimental investigation on the shear strength properties of heterogeneous discontinuities”. Geotechnical and Geological Engineering, no. 37, pp. 4959–4968 https://doi.org/10.1007/s10706-019-00955-5

Jing L, Nordlund E, Stephansson O, 1992 “An experimental study on the anisotropy and stress-dependency of the strength and deformability of rock joints”. International Journal of Rock Mechanics and Mining Sciences & Geomechanics Abstracts, no. 29, pp. 535 – 542.

Johansson F, Bagheri M, Stille H, 2010 “Variation of mechanical parameters of a slightly weathered joint in granite estimated from fourteen shear tests”. Paper presented at the ISRM International Symposium - EUROCK 2010, Lausanne, Switzerland, June 2010.

Johansson F, Stille H, 2014 “A conceptual model for the peak shear strength of fresh and unweathered rock joints”. International Journal of Rock Mechanics & Mining Sciences, no. 69, pp. 31–38. https://doi.org/10.1016/j.ijrmms.2014.03.005

Johnson RA, 2018 “Miller & Freund´s probability and statistics for engineers”. 9th ed. ISBN 10: 1-292-17601-6. Pearson Education Limited, England

Kulatilake PHSW, Shreedharan S, Sherizadeh T, Shu B, Xing Y, He P. 2016 “Laboratory Estimation of Rock Joint Stiffness and Frictional Parameters”. Geotechnical & Geological Engineering, no. 34, pp. 1723–1735. https://doi.org/10.1007/s10706-016-9984-y

Kutter KH, Otto F, 1990 “Influence of parallel and cross joints on shear behaviour of rock discontinuities”. Paper presented at International symposium on rock joints. Barton, Stephansson (eds.). A.A. Balkema, Rotterdam. ISBN 90 6191 109 5

Koyama T, Li B, Jiang Y, Jing L, 2008 “Coupled shear-flow tests for rock fractures with visualization of the fluid flow and their numerical simulations”. International Journal of Geotechnical Engineering, no. 2:3, pp. 215-227. https://doi.org/10.3328/IJGE.2008.02.03.215-227

Larsson J, Flansbjer M, Portal NW, Johnson E, Johansson F, Mas Ivars D 2020a "Geometrical Quality Assurance of Rock Joint Replicas in Shear Tests – Introductory Analysis". Paper presented at the ISRM International Symposium - EUROCK 2020, physical event not held, June.

Larsson J, Flansbjer M, 2020b “An Approach to Compensate for the Influence of the System Normal Stiffness in CNS Direct Shear Tests”. Rock Mechanics and Rock Engineering, no. 53, pp. 2185–2199. https://doi.org/10.1007/s00603-020-02051-0

Larsson J, 2021 “Experimental investigation of the system normal stiffness of a 5 MN direct shear test setup and the compensation of it in CNS direct shear tests”. IOP Conf. Ser.: Earth Environ. Sci. 833 012011. https://doi.org/10.1088/1755-1315/833/1/012011

Larsson J, Johansson F, Mas Ivars D, Johnson E, Flansbjer M, Portal NW, 2023a "A novel method for geometric quality assurance of rock joint replicas in direct shear testing – Part 1: derivation of quality assurance parameters and geometric reproducibility". Journal of Rock Mechanics and Geotechnical Engineering, no. 15, pp. 2193-2208. https://doi.org/10.1016/j.jrmge.2022.12.011.

Larsson J, Johansson F, Mas Ivars D, Johnson E, Flansbjer M, Portal NW, 2023b "A novel method for geometric quality assurance of rock joint replicas in direct shear testing – Part 2: Validation and mechanical replicability".. Journal of Rock Mechanics and Geotechnical Engineering, no. 15, pp. 2209-2223. https://doi.org/10.1016/j.jrmge.2022.12.012

Larsson J, Flansbjer M, Jacobsson L, Johansson F, Johnson E, Mas Ivars, D, Pérez-Rey I, 2025a "A three-factor experimental scale effect study on the shear strength of rock joints". *In press at Rock Mechanics and Rock Engineering.*

Larsson J, Flansbjer M, Jacobsson L, Johansson F, Johnson E, Mas Ivars D, 2025b "An experimental study on the shear stiffness of rock joints based on direct displacement measurements". *Submitted to Rock Mechanics and Geotechnical Engineering.*

Leal-Gomes MJA, 2003 "Some New Essential Questions about Scale Effects on the Mechanics of Rock Mass Joints". ISRM 2003–Technology roadmap for rock mechanics, South African Institute of Mining and Metallurgy.

Lee YK, Park JW, Song JJ, 2014 "Model for the shear behavior of rock joints under CNL and CNS conditions". International Journal of Rock Mechanics and Mining Sciences, no. 70, pp. 252-263. https://doi.org/10.1016/j.ijrmms.2014.05.005

Leichnitz W, 1985 "Mechanical properties of rock joints". International Journal of Rock Mechanics and Mining Sciences and Geomechanics Abstracts, no. 22(5), pp. 313-321.

Liu Q, Tian Y, Ma H, 2018 "Experimental investigation of the peak shear strength criterion based on three-dimensional surface description". Rock Mechanics and Rock Engineering, no. 51, pp. 1005-1025. https://doi.org/10.1007/s00603-017-1390-0

MacDonald NR, Packulak TRM, Day JJ, 2023 "A Critical Review of Current States of Practice in Direct Shear Testing of Unfilled Rock Fractures Focused on Multi-Stage and Boundary Conditions". Geosciences, no. 13:172. https://doi.org/10.3390/geosciences13060172

Muralha J, Pinto da Cunha A, 1990a "Analysis of scale effects in joint mechanical behaviour". Paper presented at the First international workshop on scale effects in rock masses. Pinto da Cunha (ed.). A.A. Balkema, Rotterdam. ISBN 90 6191 126 5

Muralha J, Pinto da Cunha A, 1990b "About LNEC experience on scale effects in mechanical behaviour". First international workshop on scale effects in rock masses. Pinto da Cunha (ed.). A.A. Balkema, Rotterdam. ISBN 90 6191 126 5

Muralha J, Grasselli G, Tatone B, Blümel M, Chryssanthakis P, Yujing J, 2014 "ISRM Suggested Method for Laboratory Determination of the Shear Strength of Rock Joints Revised Version". Rock Mechanics and Rock Engineering, no. 47, pp. 291-302 https://doi.org/10.1007/s00603-013-0519-z

Ohnishi Y, Herda H, Yoshinaka R, 1993 "Shear strength scale effect and the geometry of single and repeated rock joints". Paper presented at the Second international workshop on scale effects in rock masses. Pinto da Cunha (ed.). Balkema, Rotterdam. ISBN 90 5410 322 1

Packulak, TRM, Day JJ, Mark SD, 2018 "Practical Aspects of Boundary Condition Selection on Direct Shear Laboratory Tests".. Paper presented at the ISRM European Rock Mechanics Symposium - EUROCK 2018, St. Petersburg, Russia, May 2018

Patton FD, 1966 "Multiple modes of shear failure in rock". Paper presented at the 1st ISRM Cong. September 25–October 1, 1966, Lisbon, Portugal

Pérez Rey I, F Johansson, D Mas Ivars, H Kasani, J Larsson, L Jacobsson, M Flansbjer, (2024) Fracture parametrisation for repository design and post-closure analysis (Post), phase 2, 3 and 4 – Final Report. SKB R-24-10, Svensk Kärnbränslehantering AB, Stockholm, *to be published*

Pinto da Cunha A, 1991 "Scale effects in the determination of mechanical properties of joints and rock masses". Paper presented at the 7th ISRM Congress, Aachen, Germany, September 1991.

Ríos-Bayona F, Johansson F, Mas-Ivars D, 2021 "Prediction of Peak Shear Strength of Natural, Unfilled Rock Joints Accounting for Matedness Based on Measured Aperture". Rock Mechanics and Rock Engineering, no. 51, pp. 1533–1550. https://doi.org/10.1007/s00603-020-02340-8

Rosso RS, 1976 "A comparison of joint stiffness measurements in direct shear, triaxial compression, and In Situ". International Journal of Rock Mechanics and Mining Sciences & Geomechanics Abstracts 13:167-172 https://doi.org/10.1016/0148-9062(76)91282-1

Siren T, Hakala M, Valli J, Christiansson R, Mas Ivars D, Lam T, Mattila J, Suikkanen J, 2017 "Parametrisation of Fractures - Final Report", Posiva Report 2017-1, Posiva OY, Eurajoki, Finland

SPSS, 2023, Version 29.0.1.0 (171), IBM SPSS Statistics, https://www.ibm.com/products/spss-statistics

Um J, 1997 "Accurate quantification of rock joint roughness and development of a new peak shear strength criterion for joints". Dissertation at The University of Arizona

Uotinen L, Torkan M, Baghbanan A, Hernández EC, Rinne M, 2021 "Photogrammetric Prediction of Rock Fracture Properties and Validation with Metric Shear Tests". Geosciences, no: 11:293. https://doi.org/10.3390/geosciences11070293

Weisstein, EW, 2008 Lanczos sigma factor. From *Mathworld*, A Wolfram Web Resource. http://mathworld.wolfram.com/LanczosSigmaFactor.html (accessed 20 November 2024).

Yang ZY, Lo SC, 1997 "An index for describing the anisotropy of joint surfaces". International Journal of Rock Mechanics and Mining Sciences, no. 34, pp. 1031–1044. https://doi.org/10.1016/S1365-1609(97)80012-3

Yoshinaka R, Yoshida J, Shimizu T, Arisaka S, 1991 "Scale effect in shear strength and deformability of rock joints". Paper presented at the 7th ISRM Congress. Aachen, Germany, September 1991

Zhao R, Li C, 2022 "A New Dilation Angle Model for Rocks". Rock Mechanics and Rock Engineering, no. 55, pp. 5345–5354. https://doi.org/10.1007/s00603-022-02835-6

Box 5501
SE-114 85 Stockholm
info@befoonline.org • www.befo.se
Visiting address: Storgatan 19, Stockholm
ISSN 1104-1773